Investigations of the Kaup-Boussinesq model equations for water waves

Master thesis in Applied and Computational Mathematics

Bjørn-Sverre Juliussen

Department of Mathematics
University of Bergen
June 2, 2014

Abstract

The Kaup-Boussinesq system is a coupled system of nonlinear partial differential equations which has been derived as a model for surface waves in the context of the Boussinesq scaling, and it has also been derived for an internal wave system. In this thesis, modeling properties of the Kaup-Boussinesq water-wave model are under investigation. Differential balance laws for mass, momentum and energy are considered, and we present an exact differential balance for momentum. A Kaup-Boussinesq system describing long internal waves is investigated and compared with the Gardner equation. Finally, a spectral method for the numerical discretization of the Kaup-Boussinesq system for surface waves is put forward, and shown to converge and be stable.

Acknowledgements

First of all I would like to thank my supervisor Professor Henrik Kalisch for all his help and discussions throughout the work with my thesis. His guidance and knowledge has been essential to my work, and has motivated me during the process.

I would like to thank my fellow students who have been an inspiration for me as well. Thank you for making the days at the mathematics department easier and funnier, and also for all helpful discussions. This master process would not have been the same without you guys.

Finally, thanks to my family for making my education possible and to my soon-to-be wife Reidun for inspiration and motivational support throughout this year.

Bjørn-Sverre,
June 2014.

Contents

Outline and Motivation

In this thesis, the Kaup-Boussinesq system (KB) for surface and interfacial waves is investigated. This system arises from the Euler equations of motion, which are nonlinear and difficult to solve. The system is derived by assuming that we have long waves with small amplitude, and that the fluid is irrotational so that the local fluid velocity can be written as a potential. This potential is written as an expansion in a small parameter showing explicitly the long waves assumption. Then a variety of systems are derived by keeping different terms in the expansion, and the Kaup-Boussinesq system is one of them. The reason why we call it the Kaup-Boussinesq system is that Boussinesq scaling is used in the derivation, and it was studied by Kaup [14]. It was also derived by L. J. F. Broer in 1974 [4], but in this thesis we call it the Kaup-Boussinesq system.

The system is not heavily investigated, maybe because it is linearly ill-posed (Bona 2002 [3]), but it also has an integrable Hamiltonian structure [14], and is therefore important. In [11] there is given a solution of the Kaup-Boussinesq system for internal waves, which was used as initial guess for an iterative procedure to solve the Hamiltonian system derived in [8], and this gave very good results. In Chapter 5, the given solution is used in the investigation of the KB system for internal waves. The motivation for doing this is that when solitary waves are assumed, the KB system has the same form as the Gardner equation, also known as the extended Korteweg-de Vries equation.

Altering the parameters, the solution in [11] also solves KB for surface waves, and is therefore used as exact solution for comparing with the results of the numerical procedure in Chapter 7. Motivated by the differential balance equations for general Boussinesq systems found in [1], in Chapter 4 we find the differential balance laws for mass, momentum and energy corresponding to the KB system. An exact differential balance equation for momentum is found and presented here.

The new results presented in this thesis are thus

- An exact differential balance for momentum corresponding to Kaup-Boussinesq, Chapter 4
- We find that the KB system does not describe the broadening of large-amplitude internal waves as well as the Gardner equation, Chapter 5
- We present a spectral algorithm for the numerical approximation of solutions of the KB system for surface waves, Chapter 7

The complete outline of the thesis is as follows:

In Chapter 1 we derive the governing equations of motion used in hydrodynamics using conservation properties of mass and momentum.

In Chapter 2 appropriate boundary conditions for a given wave modeling problem are introduced, and the resulting equations are linearized to obtain the important dispersion relation for linear waves. Then, the same is done for the situation of interface waves between two fluids of different density.

In Chapter 3 the nonlinearities in the resulting system of equations from Chapter 2 are retained and different models used later are presented, herein the Kaup-Boussinesq system.

In Chapter 4 conservation of mass, momentum and energy for the KB system are presented in form of differential balance equations. An exact conservation property of the balance equation for momentum is also presented in the last section.

In Chapter 5 the Kaup-Boussinesq system for internal waves are discussed. Here, KB and Gardner are compared, using phase plane diagrams and different plots of the given solutions of the systems.

In Chapter 6 we present the theory of Spectral Methods as a numerical tool needed for Chapter 7.

In Chapter 7 the Kaup-Boussinesq system is investigated for the surface wave problem. We use the numerical procedure presented in Chapter 6 with the solution given in [11] as initial condition.

Chapter 1

Fluid Mechanics

In this chapter we will introduce the basic properties and principles of fluid dynamics, and this will eventually lead us to the governing equations of fluid motion. We will first introduce the two important properties density and viscosity, that have to be taken into account in the following governing equations. Then we will introduce the governing principles, which are the conservation laws for mass and momentum. The theory is mainly based upon the book of Kundu and Cohen [7].

1.1 Fluid Properties

1.1.1 Density

The density ρ of a fluid is defined as mass per unit volume. When we talk about the density of a fluid, we think about a specific number, but this quantity depends on the pressure and the temperature involved. We call the relation between these parameters an equation of state

$$\rho = \rho(p, T).$$

Because of the warmth from the sun, the temperature is highest at the surface, and because of all the water lying on top, the pressure is largest at the bottom. The consequences of this is that the water density increases with the depth.

1.1.2 Viscosity

Another property of fluids is the viscosity. Different fluids do not flow equally fast or smooth. We know that for example ketchup and oil flow "slower" than water. The property concerning how "well" a fluid flows, we call the viscosity of a fluid. We can think of this as friction working between the fluid and the surroundings, but also between the local fluid elements.

1.2 Conservation of Mass

An important principle used to derive an equation of motion is the principle of mass conservation. That is, mass can not disappear and can not be created. If

we look at a material volume[1] $V(t)$, the mass inside does not change and the time derivative of the total mass is zero. Hence, the following can be stated

$$\frac{d}{dt}\int_{V(t)} dm = \frac{d}{dt}\int_{V(t)} \rho(\mathbf{x},t)dV = 0. \tag{1.1}$$

Here dm is a mass element and ρ is the fluid density, so that the total mass is expressed by the integral. The density $\rho(\mathbf{x},t)$ and the upcoming $u(\mathbf{x},t)$ are in general dependent of where in the fluid we are located and also dependent of time, but from now we denote it without the $\mathbf{x}$ and t for practical reasons. Using Reynolds transport theorem[2] we get

$$\frac{d}{dt}\int_{V(t)} \rho dV = \int_{V(t)} \frac{\partial \rho}{\partial t} dV + \int_{A(t)} \rho \mathbf{u}\cdot\mathbf{n} dA = 0. \tag{1.2}$$

$A(t)$ is the surface of the material volume $V(t)$, $\mathbf{u}$ is the local fluid velocity and $\mathbf{n}$ is the outward normal vector of $A(t)$.

If we look at a geometrical volume Ω, we can take the derivative inside the integral because we have a fixed boundary

$$\frac{d}{dt}\int_{\Omega} \rho \, dV = \int_{\Omega} \frac{\partial \rho}{\partial t} dV. \tag{1.3}$$

Now, change in mass given by (1.3) must be equal to the inflow through the boundaries, which is the surface integral of the flux $\rho\mathbf{u}$. Then we have

$$\int_{\Omega(t)} \frac{\partial \rho}{\partial t} dV = -\int_{\partial\Omega(t)} \rho\mathbf{u}\cdot\mathbf{n} dA, \tag{1.4}$$

and we see that it reduces to the same equation.

Now applying Gauss' divergence theorem to the resulting equation leads to

$$0 = \int_{V(t)} \frac{\partial \rho}{\partial t} dV + \int_{A(t)} \rho\mathbf{u}\cdot\mathbf{n} dA = \int_{V(t)} \Big(\frac{\partial \rho}{\partial t} + \nabla\cdot(\rho\mathbf{u})\Big) dV.$$

For the resulting integral to be possible for every point in space, we need to require

$$\frac{\partial \rho}{\partial t} + \nabla\cdot(\rho\mathbf{u}) = 0. \tag{1.5}$$

This is called the pointwise continuity equation, and it expresses the mass conservation in differential form.

[1] We distinguish between a geometrical and a material volume. A geometrical volume (also known as a control volume) is a volume that does not change it's physical shape, while a material volume is a volume containing a specific collection of fluid particles. This volume can change it's shape, but contains always the same particles.

[2] Reynolds transport theorem describes time differentiation of integrals with time dependent limits. Here the total time derivative is divided into the partial time derivative plus a term that takes into account the movement of the surface of the volume that is being integrated over.

Equation (1.5) can be simplified. Using the material derivative[3]

$$\frac{D(\cdot)}{Dt} = \frac{\partial(\cdot)}{\partial t} + \mathbf{u} \cdot \nabla(\cdot),$$

and the identity

$$\nabla \cdot (\rho \mathbf{u}) = \rho \nabla \cdot \mathbf{u} + \mathbf{u} \cdot \nabla \rho,$$

and then dividing by ρ, we get that the continuity equation (1.5) can be written as

$$\frac{1}{\rho}\frac{D\rho}{Dt} + \nabla \cdot \mathbf{u} = 0.$$

For the further work in this thesis, we can assume constant density. Then we obtain

$$\nabla \cdot \mathbf{u} = 0. \tag{1.6}$$

Since incompressibility means that the density of fluid particles does not change, this equation is called the continuity equation for incompressible flows.

1.3 Conservation of Momentum

In this section conservation of momentum eventually lead us to the Navier-Stokes momentum equation. The much used Euler equation that will be used in the later chapters is the non-viscous form of this equation. Here, the derivation is based on a material volume, but as in the last section, we obtain the same result for a geometrical volume.

The whole principle is built on the fact that Newton's second law can be stated as

$$\frac{d}{dt}\int_{V(t)} \rho(\mathbf{x},t)\mathbf{u}(\mathbf{x},t)dV = \int_{V(t)} \rho(\mathbf{x},t)\mathbf{g}dV + \int_{A(t)} \mathbf{f}(\mathbf{n},\mathbf{x},t)dA. \tag{1.7}$$

It is applied to a material volume $V(t)$ where $A(t)$ is the surface area. Here $\mathbf{g}$ is the gravitational force per unit mass, $\mathbf{f}$ is the surface force per unit area and $\mathbf{n}$ is the surface normal with outward direction. Using again Reynolds transport theorem yields

$$\int_{V(t)} \frac{\partial}{\partial t}(\rho\mathbf{u})dV + \int_{A(t)} (\rho\mathbf{u})(\mathbf{u}\cdot\mathbf{n})dA = \int_{V(t)} \rho\mathbf{g}dV + \int_{A(t)} \mathbf{f}dA. \tag{1.8}$$

This statement considers momentum changes, both inside $V(t)$ and from the motion of $A(t)$, as a result of the surface and volume forces. To obtain the momentum equation in differential form, we first use Gauss' theorem to express the surface integrals in (1.8) as volume integrals. We have

$$\int_{A(t)} (\rho\mathbf{u})(\mathbf{u}\cdot\mathbf{n})dA = \int_{V(t)} \nabla\cdot(\rho\mathbf{u}\mathbf{u})dV = \int_{V(t)} \frac{\partial}{\partial x_i}(\rho u_i u_j)dV.$$

[3]The material derivative describes change due to time and also due to the fluids motion. It is also known as the total derivative where we have a velocity field dependent on both time and space.

Before we transform the second surface integral, we need to know that the surface forces $\mathbf{f}$ have units stress, force per unit area, and have elements $f_j = n_i\tau_{ij}$, where τ is the stress tensor. Now the integral becomes

$$\int_{A(t)} \mathbf{f} dA = \int_{A(t)} n_i\tau_{ij} dA = \int_{V(t)} \frac{\partial}{\partial x_i}(\tau_{ij}) dV.$$

The integrals in (1.8) can now be moved to one side, and we need to require that the integrand is zero at every point in space. Moving the force-terms to the other side, we obtain the momentum equation in differential form

$$\frac{\partial}{\partial t} + \frac{\partial}{\partial x_i}(\rho u_i u_j) = \rho g_j + \frac{\partial}{\partial x_i}(\tau_{ij}).$$

Another way to write this is with the use of the material derivative. Writing out the product rule for the left-hand side of this equation, using the continuity equation (1.5), we obtain

$$\rho \frac{Du_j}{Dt} = \rho g_j + \frac{\partial}{\partial x_i}(\tau_{ij}). \tag{1.9}$$

We see now that the equation relates the fluid-particle acceleration and the forces working on the fluid, so it is indeed a way of writing Newton's second law.

The stress tensor is derived by combining the different quantities affecting the deformation in a fluid. This is primarily the thermodynamic pressure p, but because of the movement the viscosity leads to additional stress. The stress tensor can thus be expressed as

$$\tau_{ij} = -p\delta_{ij} + \sigma_{ij}, \tag{1.10}$$

where the first term represents the static contribution and σ_{ij} represents the dynamic viscous contribution. Investigation of σ_{ij} with consideration of thermodynamic effects, introducing material-isotropy and using stress-symmetry eventually leads to

$$\sigma_{ij} = \mu\Big(\frac{\partial u_j}{\partial x_i} + \frac{\partial u_i}{\partial x_j}\Big) + \Big(\mu_\nu - \frac{2}{3}\mu\Big)\frac{\partial u_m}{\partial x_m}\delta_{ij}. \tag{1.11}$$

For details the reader might be referred to [7]. Combining the expression for the stress-tensor (1.10) with (1.11), and putting it into the equation (1.9), we obtain

$$\rho \frac{Du_j}{Dt} = -\frac{\partial p}{\partial x_j} + \rho g_j + \frac{\partial}{\partial x_i}\left[\mu\Big(\frac{\partial u_j}{\partial x_i} + \frac{\partial u_i}{\partial x_j}\Big) + \Big(\mu_\nu - \frac{2}{3}\mu\Big)\frac{\partial u_m}{\partial x_m}\delta_{ij}\right], \tag{1.12}$$

which we call the Navier-Stokes momentum equation. For small temperature differences, μ and μ_v can be taken outside the brackets, obtaining

$$\rho \frac{Du_j}{Dt} = -\frac{\partial p}{\partial x_j} + \rho g_j + \mu\frac{\partial^2 u_j}{\partial x_i^2} + \Big(\mu_\nu + \frac{1}{3}\mu\Big)\frac{\partial}{\partial x_j}\frac{\partial u_m}{\partial x_m}.$$

For incompressible fluids, using (1.6), we obtain the incompressible Navier-Stokes equation

$$\rho \frac{D\mathbf{u}}{Dt} = -\nabla p + \rho \mathbf{g} + \mu \nabla^{\mathbf{2}} \mathbf{u}.$$

Far from the boundaries of the flow field, we can neglect the viscosity. Then we can simplify further to obtain

$$\frac{D\mathbf{u}}{Dt} = -\frac{1}{\rho} \nabla p - g\mathbf{k}. \tag{1.13}$$

This equation (1.13) is the inviscid Navier-Stokes equation, also called the Euler equation. Throughout this section it is assumed that the wave frequency is much higher than the Coriolis frequency, so the waves are unaffected by the earth's motion. If this was not the case, the Navier-Stokes equation would include another term as well, taking into account the earth's rotation. The continuity equation (1.6) and the Euler equation for conservation of momentum (1.13) are the two equations we use later on.

Chapter 2

Wave Theory

The purpose of this chapter is to give an introduction to wave theory. We are working with gravitational waves, which means that we have waves that can be put into motion and the gravitational force will then try to put the wave back into its equilibrium position. First, using the equations of motion derived in Chapter 1, we introduce the wave function and the appropriate boundary conditions and arrive at a set to solve the velocity potential ϕ and the wave function η. Linearizing of this set give us the dispersion relation for linear waves. At the end we will look at have the problem alters when we consider internal waves. The theory in this chapter is based on the books of Whitham [18] and Kundu and Cohen [7].

2.1 Equations of motion and Boundary Conditions

Throughout this chapter it will be assumed that we have an inviscid, incompressible fluid in a constant gravitational field. The fundamental equations for fluid flow comes from the principles of conservation of mass and conservation of momentum, which eventually leads to the Euler equations. The equations (1.6) and (1.13) from Chapter 1

$$\nabla \cdot \mathbf{u} = 0, \tag{2.1}$$

$$\frac{D\mathbf{u}}{Dt} = \frac{1}{\rho}\nabla p - g\mathbf{k}, \tag{2.2}$$

are used here, with the help of boundary conditions, to find a set of equations for the wave function and the velocity potential. In many applications, these equations are more complex than necessary. Consequently there have been made many approximate models to solve the wave motion. In the next chapter we will look at some of these models. First however, appropriate boundary conditions are introduced.

Since we want to model waves, we are interested in the wave function η, as well as $\mathbf{u}$, ρ and p. If we, for example, were to have linear waves, we would get sinusoidal solutions from the linearized equations of the wave motion. A

one-dimensional traveling wave would be of the form

$$\eta(x,t) = a\cos(kx - \omega t), \tag{2.3}$$

where a is the amplitude of the wave, k is the wave number and ω is the wave frequency. Figure 2.1 shows the geometrical setup of such a wave. Generally, however, the wave function is more complicated due to nonlinearities and dispersion.

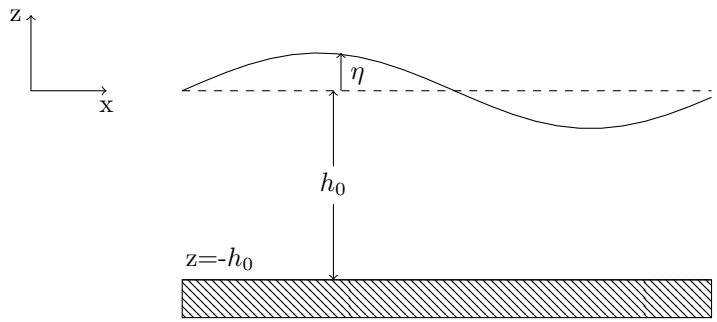

Figure 2.1: Geometric setup of the problem. Here η is the displacement from the rest position of the free surface.

In order to describe the wave function, we need to take a look at the boundary conditions for the problem. A property of the water surface is that water does not cross it. Therefore, the velocity of the surface normal to itself must be the same as the velocity of the fluid normal to the surface. This is the kinematic boundary condition, and we have

$$(\mathbf{n} \cdot \mathbf{u})_{z=\eta} = \mathbf{n} \cdot \mathbf{U}_s. \tag{2.4}$$

Here $\mathbf{n}$ is the surface normal, $\mathbf{u}$ is the local fluid velocity and $\mathbf{U}_s$ is the velocity of the surface. If we describe the surface by $f(x,y,z,t) = 0$, we get the surface normal given by

$$\mathbf{n} = \frac{\nabla f}{|\nabla f|}.$$

The velocity of the surface itself $\mathbf{n} \cdot \mathbf{U}_s = -f_t$ and $\mathbf{u} = [u,v,w]$, then (2.4) becomes

$$uf_x + vf_y + wf_z + f_t = 0.$$

This is the same as the material derivative of f being zero

$$\frac{Df}{Dt} = \frac{\partial f}{\partial t} + \nabla \cdot \mathbf{u} = 0$$

which shows that the particles on the surface stays there. We can also write this in another way. Using that the surface η is given by $z = \eta(x,y,t)$, then $f(x,y,z,t) = \eta(x,y,t) - z$, and the boundary condition becomes

$$\frac{D\eta}{Dt} = \eta_t + u\eta_x + v\eta_y - w = 0 \tag{2.5}$$

We also have a dynamic boundary condition. It states that the forces on both sides of the boundary have to be equal. This means that, the pressure in the air and in the water must be equal on the surface. To find an expression for this boundary condition, we need to go back to the Euler equation (2.2).

If we introduce the vorticity $\omega = curl(\mathbf{u})$, which says something about how the fluid particles rotates, we could rewrite equation (2.2) like

$$\frac{\partial \mathbf{u}}{\partial t} + \nabla(\frac{1}{2}\mathbf{u}^2) + \omega \times \mathbf{u} = -\frac{1}{\rho}\nabla p - g\mathbf{k}. \tag{2.6}$$

In most cases, we can assume that the flow is irrotational, that is $\omega = curl(\mathbf{u}) = 0$. Since typical problems with water waves concerns propagation into water at rest or into a uniform stream, we can argue that $\omega = 0$. We restrict ourselves to these types of problems, where we assume irrotational waves. Hence, we can introduce a velocity potential ϕ where $\mathbf{u} = \nabla\phi$, since $curl(\mathbf{u}) = \nabla \times (\nabla\phi) = 0$. Using this in equation (2.6), and integrating with respect to $\mathbf{x}$, we get

$$\frac{p - p_0}{\rho} = C(t) - \phi_t - \frac{1}{2}(\nabla\phi)^2 - gz,$$

where p_0 is the pressure in undisturbed air and C(t) is a constant of integration that can be ignored if we introduce a new potential $\phi' = \phi - \int C(t)dt$. Then we get

$$\frac{p - p_0}{\rho} = -\phi_t - \frac{1}{2}(\nabla\phi)^2 - gz.$$

Putting $p = p_0$ and using $\mathbf{u} = \nabla\phi$ in equation (2.5), the two boundary conditions at the free surface are

$$\left.\begin{aligned} \eta_t + \phi_x\eta_x + \phi_y\eta_y &= \phi_z \\ \phi_t + \tfrac{1}{2}(\phi_x^2 + \phi_y^2 + \phi_z^2) + g\eta &= 0 \end{aligned}\right\} \text{ on } z = \eta(x, y, t), \tag{2.7}$$

where the last one is the dynamic. We also have a boundary condition at the bottom. Assuming that the bottom is flat and solid, the vertical velocity must be zero and we have $\mathbf{n} \cdot \nabla\phi = 0$, where $\mathbf{n} = [0, 0, 1]$. This means that

$$\phi_z = 0, \text{ at } z = -h_0. \tag{2.8}$$

where h_0 is the distance from the averaged surface. Since we have $\mathbf{u} = \nabla\phi$, we use equation (2.1) to obtain

$$\nabla^2\phi = 0, \tag{2.9}$$

so the velocity potential must satisfy the Laplace equation. This equation and the boundary conditions (2.7) and (2.8) gives us a set of equations to find the velocity potential ϕ and the wave function η

$$\begin{aligned} \phi_{xx} + \phi_{yy} + \phi_{zz} &= 0, \quad -h_0 < z < \eta(x, y, t), \\ \phi_z &= 0, \quad z = -h_0, \\ \eta_t + \phi_x\eta_x + \phi_y\eta_y &= \phi_z, \quad z = \eta(x, y, t) \\ \phi_t + \frac{1}{2}(\phi_x^2 + \phi_y^2 + \phi_z^2) + g\eta &= 0, \quad z = \eta(x, y, t). \end{aligned} \tag{2.10}$$

2.2 Linearization and the Dispersion Relation

An important property about water waves is that they are dispersive, which means that they spread out as they travel. Waves of different wave lengths travels at different speeds. Here, we will show how the important dispersion relation, which shows how the angular frequency ω and the wave number κ are related, is obtained for linear surface waves. To make the problem linear, we first linearize our boundary conditions (2.7). If we have water at rest, then for small changes in the wave amplitude they become

$$\begin{aligned} \eta_t &= \phi_z, \\ \phi_t + g\eta &= 0. \end{aligned} \tag{2.11}$$

Differentiation of the second equation with respect to t, substituting the first one into it, we get

$$\phi_{tt} + g\phi_z = 0.$$

Since we have small perturbations on the waves initially at rest, we assume that $\eta \ll 1$ and $\phi \ll 1$, and we can apply these boundary conditions on $z = 0$ rather than on $z = \eta$. Now we have a set of equations independent of η

$$\begin{aligned} \phi_{xx} + \phi_{yy} + \phi_{zz} = 0, \text{ on } -h_0 < z < 0 \\ \phi_{tt} + g\phi_z = 0, \text{ on } z = 0 \\ \phi_z = 0, \text{ on } z = -h_0 \end{aligned} \tag{2.12}$$

Solving for ϕ, the wave function can be found from (2.11)

$$\eta(x, y, t) = -\frac{1}{g}\phi_t(x, y, 0, t) \tag{2.13}$$

2.2.1 Dispersion Relation

The elementary sinusoidal wave function of water waves, slightly more general than (2.3), is of the form

$$\eta(\mathbf{x}, t) = Ae^{i\kappa\cdot\mathbf{x} - i\omega t}, \tag{2.14}$$

and because of the equations (2.11), we seek a solution of the velocity potential in the form

$$\phi(\mathbf{x}, t) = F(z)e^{i\kappa\cdot\mathbf{x} - i\omega t}. \tag{2.15}$$

Using the Laplace equation, we get

$$F'' - \kappa^2 F = 0. \tag{2.16}$$

Using the last of the equations (2.12), equation (2.15) gives that $F'(-h_0) = 0$, which again means that

$$F \propto \cosh(\kappa(h_0 + z)),$$

from equation (2.16). Putting the equation for the wave function (2.14) and velocity potential (2.15) into the relation (2.13), we get

$$A = \frac{i\omega}{g}F(0).$$

Then F can be written like

$$F(z) = -\frac{igA}{\omega}\frac{\cosh(\kappa(h_0+z))}{\cosh(\kappa h_0)},$$

and ϕ becomes

$$\phi = -\frac{igA}{\omega}\frac{\cosh(\kappa(h_0+z))}{\cosh(\kappa h_0)}e^{i\kappa\cdot\mathbf{x}-i\omega t}.$$

The remaining boundary condition, the second of equations (2.12) $\phi_{tt}+g\phi_z = 0$, and a little manipulation now gives us

$$\omega^2 = g\kappa\tanh(\kappa h_0), \tag{2.17}$$

which we call the dispersion relation for linear surface waves. The phase speed of a wave is given by

$$c = \frac{\omega}{\kappa}.$$

If c is constant we do not have dispersion. If however, c is dependent of κ, which is generally the case, we will have dispersion.

2.3 Internal waves

So far, the theory described is for a water surface with a layer of air above it. The case becomes a little different when we assume that there is water with a different density above this surface. In the ocean, solar heating creates a sharp-density gradient, so that we get a well defined interface between the warmer upper layer and the colder lower layer, and we get internal waves at the interface. This is also the case in an estuary or in a fjord. Here the fresh river water flows into the salty ocean water. The lighter fresh water lies on top of the heavier ocean water, because the river water is less saline and consequently lighter. We can no longer ignore the changes in pressure above the surface. We now consider two fluids with pressure p_1 and p_2 and density ρ_1 and ρ_2. The geometrical setup is shown in Figure 2.2.

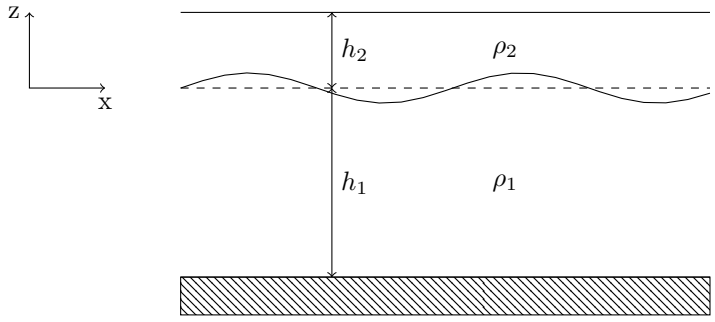

Figure 2.2: Geometric setup of the internal waves problem. We set $z = 0$ at the interface.

In the same manner as for surface waves, we have a kinematic boundary condition saying that water can not cross the surface. The condition is the

same, stating that the velocity of the interface normal to itself must be the same as the velocity of the fluid normal to the interface

$$(\mathbf{n}\cdot\mathbf{u})_{z=\eta} = \mathbf{n}\cdot\mathbf{U}_s,$$

only now, this must be the same for both fluids. The dynamic boundary condition is also the same, stating that the pressure in both fluids must be equal on the interface, $p_1 = p_2$. We write equation (2.2) as (2.6) for the two different fluids. Again irrotationality is assumed and a velocity potential $\mathbf{u} = \nabla\phi$ is introduced. We integrate with respect to $\mathbf{x}$, and now get the two equations

$$\begin{aligned} p_1 - p_0 &= -\rho_1(\phi_{1_t} + \tfrac{1}{2}(\bigtriangledown\phi_1)^2 + gz), \\ p_2 - p_0 &= -\rho_2(\phi_{2_t} + \tfrac{1}{2}(\bigtriangledown\phi_2)^2 + gz), \end{aligned} \tag{2.18}$$

where p_0 is the common undisturbed pressure value. Putting $p_1 = p_2$, the new boundary conditions are

$$\left.\begin{aligned} \rho_1(\phi_{1_t} + \tfrac{1}{2}(\nabla\phi_1)^2 + gz) &= \rho_2(\phi_{2_t} + \tfrac{1}{2}(\nabla\phi_2)^2 + gz) \\ \eta_t + \phi_{1_x}\eta_x + \phi_{1_y}\eta_y &= \phi_{1_z} \\ \eta_t + \phi_{2_x}\eta_x + \phi_{2_y}\eta_y &= \phi_{2_z} \end{aligned}\right\} \text{on } z = \eta(x,y,t). \tag{2.19}$$

In addition, the two velocity potentials must also satisfy the Laplace equation, as a consequence of the continuity equation (2.1).

The dispersion relation for internal waves is a bit more complicated than the surface wave case. For the simplest case, when we can assume that the interface lies between two infinite deep fluids, we get

$$\phi_1 \to 0 \text{ as } z \to \infty, \quad \text{and} \quad \phi_2 \to 0 \text{ as } z \to -\infty,$$

and when motion in the y-direction is ignored, we have that

$$\frac{\partial^2\phi_1}{\partial x^2} + \frac{\partial^2\phi_1}{\partial z^2} = 0 \ , \ \frac{\partial^2\phi_1}{\partial x^2} + \frac{\partial^2\phi_1}{\partial z^2} = 0.$$

Then the elementary solution is of the form

$$\eta = ae^{i(\kappa x - \omega t)},$$

$$\phi_1 = b_1 e^{i(\kappa x-\omega t)-\kappa z}, \qquad \phi_2 = b_2 e^{i(\kappa x-\omega t)+\kappa z}.$$

The dispersion relation is now found from the boundary conditions (2.19), and after some calculations we get

$$\omega = \sqrt{g\kappa\Big(\frac{\rho_2 - \rho_1}{\rho_1 + \rho_2}\Big)}.$$

We observe that when $\rho_1 \approx 0$ we get $\omega = \sqrt{g\kappa}$, which agrees with the dispersion relation for linear surface waves (2.17) when we have deep water, such that $\tanh(\kappa h_0) \approx 1$.

Chapter 3

Nonlinear Model Equations

To solve the nonlinear set of equations for ϕ and η obtained in the preceding chapter, we make certain simplifications to obtain model equations. There are many ways to make such simplifications, and here we will derive some of the most common nonlinear model equations. Generally, to model surface waves, the variables at interest are the local wave velocity at the surface u, and the wave function η. The resulting model equations therefore contains these variables. In the first section, the shallow water equations are derived, which makes the foundation for higher order nonlinear models. In the second section, dispersive effects are incorporated into the shallow water theory. This eventually leads to systems like Kaup-Boussinesq and the Korteweg-deVries equation. The theory is based on the book of Whitham [18] and the article of Bona, Chen and Saut [3].

3.1 Shallow Water Theory

When we consider shallow water it means we assume that $\kappa h_0 \to 0$, or $\frac{h_0}{\lambda} \to 0$, since $\kappa = \frac{2\pi}{\lambda}$. This means that the undisturbed water depth h_0 is small compared to the wavelength, so we either have shallow water or long waves, or even both. From the preceding chapter, we have the dispersion relation for linear waves given by

$$\omega^2 = g\kappa \tanh(\kappa h_0).$$

Using the approximation $\kappa h_0 \to 0$, $\tanh(\kappa h_0) \to \kappa h_0$, this makes the dispersion relation

$$\omega^2 \sim g h_0 \kappa^2. \tag{3.1}$$

The phase velocity $c = \frac{\omega}{\kappa} = \sqrt{g h_0}$ is independent of κ. The dispersive effects is therefore not taken into account here.

To get the equations for shallow water, we write out the Euler equation (2.2) in component form and approximate. The vertical component is

$$-\frac{1}{\rho}\frac{\partial p}{\partial z} - g = 0. \tag{3.2}$$

We integrate it to get

$$p - p_0 = \rho g(\eta - z). \tag{3.3}$$

The two horizontal components are given by

$$\frac{\partial u_i}{\partial t} + u\frac{\partial u_i}{\partial x} + v\frac{\partial u_i}{\partial y} + w\frac{\partial u_i}{\partial z} = -\frac{1}{\rho}\frac{\partial p}{\partial x_i}$$

where $i = 1, 2$ and the velocity $\mathbf{u} = [u, v, w]$. Since (3.3) gives $p_{x_i} = \rho g \eta_{x_i}$, we get

$$\frac{\partial u_i}{\partial t} + u\frac{\partial u_i}{\partial x} + v\frac{\partial u_i}{\partial y} + w\frac{\partial u_i}{\partial z} = -g\frac{\partial \eta}{\partial x_i}$$

Since the surface displacement η is independent of z, then the change of the velocity following a particle is also independent of z, hence

$$\frac{\partial u_i}{\partial t} + u\frac{\partial u_i}{\partial x} + v\frac{\partial u_i}{\partial y} + g\frac{\partial \eta}{\partial x_i} = 0 \tag{3.4}$$

The equation (2.1) for incompressible flow gives that $u_x + v_y + w_z = 0$, which, when integrated over the depth, becomes

$$\begin{aligned} 0 =& \int_{-h_0}^{\eta} \left(\frac{\partial u}{\partial x} + \frac{\partial v}{\partial y} + \frac{\partial w}{\partial z}\right) dz \\ =& \frac{\partial}{\partial x}\int_{-h_0}^{\eta} u dz - [u]_{z=\eta}\frac{\partial \eta}{\partial x} - [u]_{z=-h_0}\frac{\partial h_0}{\partial x} \\ &+ \frac{\partial}{\partial y}\int_{-h_0}^{\eta} v dz - [v]_{z=\eta}\frac{\partial \eta}{\partial y} - [v]_{z=-h_0}\frac{\partial h_0}{\partial y} + [w]_{z=-h_0}^{z=\eta} \end{aligned}$$

where Leibniz integral rule [1] is used twice to obtain the second equality. Using the boundary conditions (2.10) we get

$$\frac{\partial}{\partial x}\int_{-h_0}^{\eta} u dz + \frac{\partial}{\partial y}\int_{-h_0}^{\eta} v dz + \frac{\partial \eta}{\partial t} = 0.$$

And since u and v are independent of z, we obtain

$$\frac{\partial \eta}{\partial t} + h_0\frac{\partial u}{\partial x} + h_0\frac{\partial v}{\partial y} + \frac{\partial}{\partial x}(\eta u) + \frac{\partial}{\partial y}(\eta v) = 0. \tag{3.5}$$

The equations (3.4) and (3.5) are called the shallow water equations for η and $\mathbf{u}$. They provide a nonlinear set for shallow water or long waves. For one-dimensional waves, the equations can be written

$$\begin{aligned} \eta_t + h_0 u_x + (u\eta)_x = 0, \\ u_t + u u_x + g\eta_x = 0. \end{aligned}$$

3.2 Inclusion of dispersion

In this section, dispersive effects are considered and we arrive at the Kaup-Boussinesq system and the Korteweg-deVries-equation. If we write $\tanh\kappa h_0$ in

[1] The Leibniz Integral rule is a differentiation rule, and it states that $\frac{\partial}{\partial z}\int_{a(z)}^{b(z)} f(x,z)dx = \int_{a(z)}^{b(z)} \frac{\partial f}{\partial z}dx + f(b(z),z)\frac{\partial b}{\partial z} - f(a(z),z)\frac{\partial a}{\partial z}$. This is necessary because the integral limits are functions of the differential variable.

the dispersion relation as a Taylor series expansion about $\kappa = 0$, the systems corresponds to the inclusion of another term in this expansion

$$\omega^2 = c_0^2\kappa^2 - \frac{1}{3}c_0^2 h_0^2 \kappa^4,$$

where the relation $c_0 = \sqrt{gh_0}$ is used. To do this, we write the velocity potential as an expansion in the parameter $\beta = \frac{h_o^2}{l^2}$, called the dispersion parameter. We also introduce the parameter $\alpha = \frac{a}{h_0}$, which occurs in connection with the nonlinear terms and is therefore called the nonlinear parameter. In the following, it will be assumed that there is an approximate balance between nonlinearity and dispersiveness. This is done by assuming $\alpha \sim \beta$, $\alpha \ll 1$ and $\beta \ll 1$ and keeping terms in α and β up to the same order. This is called the Boussinesq scaling.

First, we remember the system from the preceding chapter (2.10) consisting of the boundary conditions and Laplace equation for the velocity potential

$$\begin{aligned} \phi_{xx} + \phi_{yy} + \phi_{zz} = 0, &\quad -h < z < \eta(x,y,t), \\ \phi_z = 0, &\quad z = -h_0, \\ \eta_t + \phi_x\eta_x + \phi_y\eta_y = \phi_z, &\quad z = \eta(x,y,t) \\ \phi_t + \frac{1}{2}(\phi_x^2 + \phi_y^2 + \phi_z^2) + g\eta = 0, &\quad z = \eta(x,y,t). \end{aligned} \tag{3.6}$$

Now, we assume that we are working in an open channel where the fluid is uniform in the cross-channel direction, say for example the y-direction, which means we neglect motion in this direction. We also normalize the variables such that they are of order one, and terms can be ordered explicitly in expansions with respect to the small parameters α and β, showing the assumptions about small amplitude and long wavelength. We normalize them in the following way

$$\begin{aligned} x = l\tilde{x}, \quad z = h_0(\tilde{z} - 1), \quad t = \tfrac{l\tilde{t}}{c_0}, \\ \eta = a\tilde{\eta}, \quad \phi = \tfrac{gla\tilde{\phi}}{c_0}. \end{aligned} \tag{3.7}$$

Using the normalized variables we see that the parameters α and β occurs, and the system (3.6) becomes

$$\begin{aligned} \beta\phi_{xx} + \phi_{zz} = 0, &\quad 0 < z < 1 + \alpha\eta, \\ \phi_z = 0, &\quad z = 0, \\ \eta_t + \alpha\phi_x\eta_x - \frac{1}{\beta}\phi_z = 0, &\quad z = 1 + \alpha\eta, \\ \eta + \phi_t + \frac{1}{2}\alpha\phi_x^2 + \frac{1}{2}\frac{\alpha}{\beta}\phi_z^2 = 0, &\quad z = 1 + \alpha\eta. \end{aligned} \tag{3.8}$$

Here, the tildes on the normalized variables are removed for practical reasons. The next step is to represent ϕ as an expansion,

$$\phi(x,z,t) = \sum_{n=0}^{\infty} z^n f_n(x,t)$$

This way of writing the expansion is supported by the assumption that for small depth, ϕ_x is practically independent of z. From Laplace's equation, we get

$$\sum_{n=0}^{\infty}(n+1)(n+2)z^n f_{n+2}(x,t) = -\sum_{n=0}^{\infty}\beta z^n (f_n(x,t))_{xx}.$$

We use the resulting recurrence relation for f

$$(n+1)(n+2)f_{n+2}(x,t) = -\beta(f_n(x,t))_{xx},$$

and the condition $\phi_z = 0$ on $z = 0$ from (3.8), to obtain

$$\phi = \sum_{n=0}^{\infty}(-1)^n \frac{z^{2n}}{(2n)!}\frac{\partial^{2n} f}{\partial x^{2n}}\beta^n, \tag{3.9}$$

where $f = f_0$. Substituting this into the surface conditions, the last two of the equations (3.8), and putting $z = 1 + \alpha\eta$, we obtain

$$\begin{aligned}\eta_t + \alpha\eta_x \sum_{n=0}^{\infty}\Big(\frac{(-1)^n}{(2n)!}\frac{\partial^{2n+1} f}{\partial x^{2n+1}}(1+\alpha\eta)^{2n}\Big)\beta^n \\ + \sum_{n=0}^{\infty}\Big(\frac{(-1)^n}{(2n+2)!}\frac{\partial^{2n+2} f}{\partial x^{2n+2}}(1+\alpha\eta)^{2n+1}\Big)\beta^n = 0,\end{aligned} \tag{3.10}$$

and

$$\begin{aligned}\eta + \sum_{n=0}^{\infty}\Big(\frac{(-1)^n}{(2n)!}\frac{\partial^{2n+1} f}{\partial x^{2n}\partial t}(1+\alpha\eta)^{2n}\Big)\beta^n \\ + \frac{1}{2}\alpha\Big(\sum_{n=0}^{\infty}\frac{(-1)^n}{(2n)!}\frac{\partial^{2n+1} f}{\partial x^{2n+1}}(1+\alpha\eta)^{2n}\beta^n\Big)^2 \\ + \frac{1}{2}\alpha\beta\Big(\sum_{n=0}^{\infty}\frac{(-1)^n}{(2n+2)!}\frac{\partial^{2n+2} f}{\partial x^{2n+2}}(1+\alpha\eta)^{2n+1}\beta^n\Big)^2 = 0,\end{aligned} \tag{3.11}$$

From this we obtain several different systems by keeping terms in α and β of different orders. In the following we will see how to obtain the Kaup-Boussinesq system and the Korteweg-deVries equation from these equations. The shallow water equations can also be obtained from here keeping first order terms of α.

3.2.1 The Kaup-Boussinesq system

To get the second order approximating Boussinesq systems, we keep the first terms in the series in the equations (3.10) and (3.11) up to second order in α and β, writing the rest of the series expansions as simply "cubic terms" on the right-hand side. Expanding the powers of $z = (1 + \alpha\eta)$, writing the resulting higher order terms together with the rest terms of cubic terms, we obtain

$$\begin{aligned}\eta_t + \alpha\eta_x(\frac{\partial f}{\partial x} - \frac{1}{2}\frac{\partial^3 f}{\partial x^3}\beta) + \frac{\partial^2 f}{\partial x^2} + \alpha\eta\frac{\partial^2 f}{\partial x^2} \\ -\frac{1}{6}\frac{\partial^4 f}{\partial x^4}(1+3\alpha\eta)\beta + \frac{1}{5!}\frac{\partial^6 f}{\partial x^6}\beta^2 = \text{cubic terms},\end{aligned}$$

and

$$\eta + \frac{\partial f}{\partial t} - \frac{1}{2}\frac{\partial^3 f}{\partial x^2 \partial t}(1 + 2\alpha\eta)\beta + \frac{1}{4!}\frac{\partial^5 f}{\partial x^4 \partial t}\beta^2$$

$$+\frac{1}{2}\alpha(\frac{\partial f}{\partial x})^2 - \frac{1}{2}\alpha\beta\frac{\partial f}{\partial x}\frac{\partial^3 f}{\partial x^3} + \frac{1}{2}\alpha\beta(\frac{\partial^2 f}{\partial x^2})^2 = \text{cubic terms.}$$

Next, differentiating the second equation with respect to x, and approximating the scaled horizontal velocity at the bottom u with $\frac{\partial f}{\partial x}$, yields

$$\begin{aligned}\eta_t + u_x + \alpha\eta_x u + \alpha\eta u_x - \tfrac{1}{6}\beta u_{xxx} - \tfrac{1}{2}\alpha\beta\eta_x u_{xx} \\ -\tfrac{1}{2}\alpha\beta\eta u_{xxx} + \tfrac{1}{120}\beta^2 u_{xxxxx} = \text{cubic terms,}\end{aligned} \tag{3.12}$$

$$\begin{aligned}\eta_x + u_t - \tfrac{1}{2}\beta u_{xxt} + \alpha u u_x - \alpha\beta\eta u_{xxt} - \alpha\beta\eta_x u_{xt} + \tfrac{1}{2}\alpha\beta u_x u_{xx} \\ -\tfrac{1}{2}\alpha\beta u u_{xxx} + \tfrac{1}{24}\beta^2 u_{xxxxt} = \text{cubic terms.}\end{aligned} \tag{3.13}$$

Since we are interested in the velocity at the surface, using w as the scaled horizontal velocity at the surface $z = 1$, we want to base our model on w and η rather than u and η. Approximating w with the velocity potential (3.9) up to second order in β yields

$$w = \phi_x|_{z=1} = u - \frac{1}{2}\beta u_{xx} + \frac{1}{4!}\beta^2 u_{xxxx} + O(\beta^3),$$

where $u = f_x$ is used. Now we have a relation between w and u, and we want to express u in terms of w, so that we can substitute this into the equations (3.12) and (3.13). Using the continuous Fourier transform we can do this. In Fourier space, we get the relation

$$\hat{w} = (1 + \frac{1}{2}\beta k^2 + \frac{1}{4!}\beta^2 k^4)\hat{u} + O(\beta^3).$$

Here, the hats denotes the Fourier transform of the variables, and k are the different wave numbers in the Fourier approximation. Now we can divide by the Fourier multiplier, and obtain

$$\hat{u} = (1 + \frac{1}{2}\beta k^2 + \frac{1}{4!}\beta^2 k^4)^{-1}\hat{w} + O(\beta^3)$$

$$= (1 - \frac{1}{2}\beta k^2 + \frac{5}{24}\beta^2 k^4)\hat{w} + O(\beta^3).$$

Hence, we can write

$$u = w + \frac{1}{2}\beta w_{xx} + \frac{5}{24}\beta^2 w_{xxxx} + O(\beta^3). \tag{3.14}$$

Now, we substitute this expression for u into the system (3.12)-(3.13). If we gather all the quadratic and higher order terms in α and β on the right-hand side, we get the system

$$\begin{aligned}\eta_t + w_x + \alpha(\eta w)_x + \frac{1}{3}\beta w_{xxx} = O(\alpha\beta, \beta^2), \\ \eta_x + w_t + \alpha w w_x = O(\alpha\beta, \beta^2).\end{aligned}$$

This is called the Kaup system, or Kaup-Boussinesq due to the Boussinesq scaling used to obtain it. As earlier mentioned, this system considers both nonlinear and dispersive effects, and we can see why the parameters α and β are called the nonlinearity and the dispersive parameter respectively. Changing back to the original variables, we get the Kaup-Boussinesq system in dimensional variables

$$\begin{aligned} \eta_t + h_0 w_x + (w\eta)_x + \frac{1}{3} h_0^3 w_{xxx} = 0, \\ w_t + g\eta_x + w w_x = 0. \end{aligned} \tag{3.15}$$

Here, the second order terms in α and β are neglected.

3.2.2 The Korteweg-de Vries equation

Since the Korteweg-de Vries equation is used in Chapter 6 for checking the numerical method for an uncoupled system, we explain here shortly how this is derived. Starting with the system (3.10)-(3.11), we retain the first order terms of α and β, but drop the mixed second order terms of $O(\alpha\beta)$. Letting, in the same way as before, $u = f_x$, we get

$$\begin{aligned} \eta_t + \big((1+\alpha\eta)u\big)_x - \tfrac{1}{6}\beta u_{xxx} + O(\alpha^2, \alpha\beta, \beta^2) = 0, \\ u_t + \alpha u u_x + \eta_x - \tfrac{1}{2}\beta u_{xxt} + O(\alpha^2, \alpha\beta, \beta^2) = 0. \end{aligned} \tag{3.16}$$

By specializing to a wave moving to the right and neglecting the terms of order α and β, the system (3.16) has a solution

$$u = \eta, \quad \eta_t + \eta_x = 0.$$

Corrected to the first order of α and β, we have a solution of the form

$$\begin{aligned} u = \eta + \alpha A + \beta B + O(\alpha^2, \beta^2), \\ \eta_t + \eta_x + O(\alpha, \beta) = 0, \end{aligned} \tag{3.17}$$

where A and B are unspecified functions of η and its x derivatives. The equations (3.16) now becomes

$$\begin{aligned} \eta_t + \eta_x + \alpha(A_x + 2\eta\eta_x) + \beta(B_x - \tfrac{1}{6}\eta_{xxx}) + O(\alpha^2, \beta^2) = 0, \\ \eta_t + \eta_x + \alpha(A_t + \eta\eta_x) + \beta(B_t - \tfrac{1}{2}\eta_{xxt}) + O(\alpha^2, \beta^2) = 0. \end{aligned} \tag{3.18}$$

Using the last of the equations (3.17), we can change the t derivatives in the first order terms to negative x derivatives. For the two equations to be consistent, the terms linear in α and β must be equal. Hence, A and B must satisfy

$$A = -\frac{1}{4}\eta^2, \quad B = \frac{1}{3}\eta_{xx}.$$

Then (3.18) becomes

$$\eta_t + \eta_x + \frac{3}{2}\alpha\eta\eta_x + \frac{1}{6}\beta\eta_{xxx} + O(\alpha^2, \beta^2) = 0.$$

This is the normalized Korteweg-deVries equation. If we transform back to the original variables, and neglect the term of second order α and β, we get the normal form of the Korteweg-deVries equation

$$\eta_t + c_0(1 + \frac{3}{2}\frac{\eta}{h_0})\eta_x + \frac{1}{6}c_0 h_0^2 \eta_{xxx} = 0. \tag{3.19}$$

3.2.3 Model equations for internal wave systems

The system (3.15) applies for surface waves. A system for internal waves can also be derived, using the corresponding boundary conditions. A derivation can be found in for example [9], which is based on the boundary conditions for internal waves (2.19), but which uses a Hamiltonian system for the system of equations of motion. The Hamiltonian is given as a sum of energy integrals of the kinetic and potential energy. The derivation is quite complicated, but results in the following system

$$\begin{aligned} \eta_t + \alpha u_x + \epsilon^2(\delta u_{xxx} + \gamma(\eta u)_x) = 0, \\ u_t + \beta \eta_x + \epsilon^2 \gamma u u_x = 0, \end{aligned} \tag{3.20}$$

where the parameters α, β, δ and γ are given by

$$\alpha = \tfrac{h_1 h_2}{\rho_2 h_1 + \rho h_2}, \qquad \beta = g(\rho_1 - \rho_2),$$

$$\delta = \tfrac{1}{3}\tfrac{(h_1 h_2)^2(\rho_2 h_2 + \rho_1 h_1)}{(\rho_2 h_1 + \rho_1 h_2)^2}, \qquad \gamma = \tfrac{\rho_1 h_2^2 - \rho_2 h_1^2}{(\rho_2 h_1 + \rho_1 h_2)^2}.$$

Here, the subscript 1 denotes the lower fluid layer, and subscript 2 the upper one. The parameter ϵ arises due to a scaling of x and η, and can be put equal to 1 without influencing the system.

For comparison with Kaup Boussinesq for internal waves in Chapter 4 the Gardner equation is used. This can be found in for example [13], and is of the form

$$\eta_t + c_0\eta_x + \alpha_1 \eta\eta_x + \alpha_2 \eta^2 \eta_x + \beta_1 \eta_{xxx} = 0. \tag{3.21}$$

Here, the parameters are

$$\begin{aligned} c_0^2 = \tfrac{g h_1 h_2(\rho_1 - \rho_2)}{\rho_2 h_1 + \rho_1 h_2}, \quad \alpha_1 = \tfrac{3c_0}{2h_1 h_2}\tfrac{\rho_1 h_2^2 - \rho_2 h_1^2}{\rho_2 h_1 + \rho_1 h_2}, \\ \alpha_2 = \tfrac{3c_0}{h_1^2 h_2^2}\left[\tfrac{7}{8}(\tfrac{\rho_1 h_2^2 - \rho_2 h_1^2}{\rho_2 h_1 + \rho_1 h_2})^2 - \tfrac{\rho_2 h_1^3 + \rho_1 h_2^3}{\rho_2 h_1 + \rho_1 h_2}\right], \quad \beta = \tfrac{c_0 h_1 h_2}{6}\tfrac{\rho_1 h_1 + \rho_2 h_2}{\rho_2 h_1 + \rho_1 h_2} \end{aligned} \tag{3.22}$$

Chapter 4

Balance equations for Kaup-Boussinesq

In this chapter, conservation of mass, momentum and energy are presented for the Kaup-Boussinesq system and written as differential balance equations in the order of α and β corresponding to KB. In the last section, an exact differential balance for momentum for KB is presented. The theory here is mainly based on the article by Ali and Kalisch [1], where the balance equations are shown for a general Boussinesq system of equations, in which the KB system is a special case of. In [2] we find the differential balance for energy of KB specifically. The expressions for momentum and energy presented here are used later to confirm that the numerical method in Chapter 7 conserves these quantities over the considered region.

4.1 Shallow water

It is shown that the shallow water equations

$$\begin{aligned} \eta_t + h_0 u_x + (\eta u)_x &= 0, \\ u_t + g\eta_x + uu_x &= 0, \end{aligned}$$

features conservation of mass and momentum. We look at the volume limited by x_1 and x_2, the bottom and the moving surface, as shown in Figure 4.1. Three of the sides are fixed, while the surface is moving. Thus, this is a combined material and geometrical volume, though it can for all practical purposes can be regarded as a geometrical volume. Here, the motion in y-direction is ignored, as in the derivation of the nonlinear model equations from Chapter 3. Since no mass leaves the surface, the only change is the flux corresponding to the two fixed lateral boundaries. The balance equations given by the mass and momentum density M and I with the fluxes q_M and q_I are then the following

$$\begin{aligned} \frac{\partial}{\partial t} M + \frac{\partial}{\partial x} q_M &= 0, \\ \frac{\partial}{\partial t} I + \frac{\partial}{\partial x} q_I &= 0. \end{aligned} \tag{4.1}$$

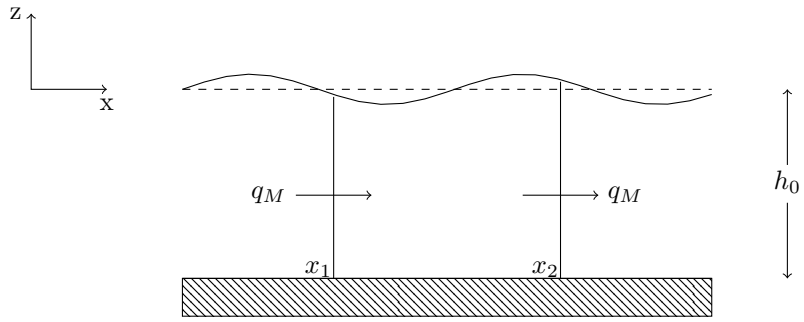

Figure 4.1: Geometric setup of the problem. The volume is limited by the bottom, the two sides at x_1 and x_2 and the moving surface. This is a combined material and geometrical volume.

Here

$$M = \rho(h_0 + \eta), \quad I = \rho(h_0 + \eta)u,$$
$$q_M = \rho(h_0 u + \eta u), \quad q_I = \rho(h_0 + \eta)u^2 + \frac{\rho}{2} g(h_0 + \eta)^2.$$

For smooth solutions, the equations (4.1) are both equal to the shallow water equations, as shown in [1]. The conservation of energy has the same form

$$\frac{\partial}{\partial t} E + \frac{\partial}{\partial x} q_E = 0,$$

here with

$$E = \frac{\rho}{2} u^2 (h_0 + \eta) + \frac{\rho}{2} g(2h_0\eta + \eta^2),$$
$$q_E = \frac{\rho}{2} u^3 (h_0 + \eta) + \rho g u (h_0 + \eta)^2.$$

We want to have corresponding balance equations for the Kaup-Boussinesq system.

4.2 Mass

For the conservation of mass, the change in mass density is given by the flux through the lateral boundaries

$$\frac{d}{dt} \int_{x_1}^{x_2} \int_{-h_0}^{\eta} \rho \, dz dx = \left[\int_{-h_0}^{\eta} \rho \, \phi_x \, dz \right]_{x_2}^{x_1}.$$

We observe that this has the same form as (1.4) in Chapter 1, except for the simplification in the y-direction. Now, however, we transform to non-dimensional variables by (3.7), integrate with respect to $\tilde{z}$, write out the expression for $\tilde{\phi}_x$ and use the relation (3.14), so that this becomes

$$\frac{d}{d\tilde{t}} \int_{x_1/l}^{x_2/l} (1 + \alpha\tilde{\eta}) d\tilde{x} = \alpha \left[\tilde{w} + \alpha \tilde{w} \tilde{\eta} + \frac{\beta}{3} \tilde{w}_{\tilde{x}\tilde{x}} + O(\alpha\beta, \alpha^2) \right]_{x_2/l}^{x_1/l}$$

Further, we divide by the length of the interval, and take the limit $x_2/l \to x_1/l$. Then the differential balance equation for mass is obtained

$$\tilde{\eta}_{\tilde{t}} + \tilde{w}_{\tilde{x}} + \alpha(\tilde{w}\tilde{\eta})_{\tilde{x}} + \frac{\beta}{3}\tilde{w}_{\tilde{x}\tilde{x}\tilde{x}} = O(\alpha\beta, \beta^2).$$

This can be written as

$$\frac{\partial}{\partial \tilde{t}}\tilde{M} + \frac{\partial}{\partial \tilde{x}}\tilde{q}_M = O(\alpha^2\beta, \alpha\beta^2), \tag{4.2}$$

when the non-dimensional mass and density are given by

$$\begin{aligned} \tilde{M} &= 1 + \alpha\tilde{\eta}, \\ \tilde{q}_M &= \alpha\tilde{w} + \alpha^2\tilde{\eta}\tilde{w} + \frac{1}{3}\alpha\beta\tilde{w}_{\tilde{x}\tilde{x}}. \end{aligned}$$

In dimensional variables, we have

$$\begin{aligned} M &= \rho(h_0 + \eta), \\ q_M &= \rho h_0 w + \rho\eta w + \frac{1}{3}\rho h_0^3 w_{xx}, \end{aligned}$$

where the scalings $M = \rho h_0 \tilde{M}$ and $q_M = \rho h_0 c_0 \tilde{q}_M$ are used. We change to dimensional variables

$$\frac{\partial}{\partial \tilde{t}}\tilde{M} + \frac{\partial}{\partial \tilde{x}}\tilde{q}_M = \frac{c_0 h_0}{l}\left(\eta_t + h_0 w_x + (\eta w)_x + \frac{1}{3}h_0^3 w_{xxx}\right) = 0.$$

The expression inside the parentheses is just the first equations of the Kaup-Boussinesq system (3.15), and thus KB conserves mass exactly.

4.3 Momentum

The momentum density $\mathcal{I}$ is given by

$$\mathcal{I} = \int_{x_1}^{x_2}\int_{-h_0}^{\eta} \rho\phi_x \, dzdx.$$

For the case of conservation, the change in momentum is equal to the flux through the boundaries plus the work done on the boundary

$$\frac{d}{dt}\int_{x_1}^{x_2}\int_{-h_0}^{\eta} \rho\phi_x \, dzdx = \left[\int_{-h_0}^{\eta} \rho\phi_x^2 \, dz + \int_{-h_0}^{\eta} P \, dz\right]_{x_2}^{x_1}.$$

The pressure used here is found in [1] to be

$$P = \rho g(\eta - z) + \frac{1}{2}\rho\big((z + h_0)^2 - h_0^2\big)w_{xt}, \tag{4.3}$$

which comes from the Bernoulli equation. The atmospheric pressure is assumed to be zero. Now transforming to non-dimensional variables and substituting the expression for $\tilde{\phi_x}$ and the expression found for the pressure P, again using

the relation (3.14), after a little manipulation the following differential balance equation is obtained

$$\tilde{w}_{\tilde{t}} + \alpha(\tilde{w}\tilde{\eta})_{\tilde{t}} + \frac{\beta}{3}\tilde{w}_{\tilde{x}\tilde{x}\tilde{t}} + \tilde{\eta}_{\tilde{x}} + 2\alpha\tilde{w}\tilde{w}_{\tilde{x}} + \alpha\tilde{\eta}\tilde{\eta}_{\tilde{x}} - \frac{1}{3}\beta\tilde{w}_{\tilde{x}\tilde{x}\tilde{t}} = O(\alpha^2, \alpha\beta, \beta^2). \quad (4.4)$$

With

$$\begin{aligned} \tilde{I} &= \alpha\tilde{w} + \alpha^2\tilde{w}\tilde{\eta} + \frac{1}{3}\alpha\beta\tilde{w}_{\tilde{x}\tilde{x}}, \\ \tilde{q}_I &= \alpha\tilde{\eta} + \alpha^2\tilde{w}^2 + \frac{1}{2}\alpha^2\tilde{\eta}^2 - \frac{1}{3}\alpha\beta\tilde{w}_{\tilde{x}\tilde{t}} + \frac{1}{2}, \end{aligned} \quad (4.5)$$

the momentum balance can be written

$$\frac{\partial}{\partial\tilde{t}}\tilde{I} + \frac{\partial}{\partial\tilde{x}}\tilde{q}_I = O(\alpha^3, \alpha^2\beta, \alpha\beta^2). \quad (4.6)$$

In dimensional form, with scalings $I = \rho h_0 c_0 \tilde{I}$ and $q_I = \rho h_0 c_0^2 \tilde{q}_I$, we get

$$\begin{aligned} I &= \rho(h_0 + \eta)w + \frac{1}{3}\rho h_0^3 w_{xx}, \\ q_I &= \rho h_0 w^2 + \frac{1}{2}\rho g(h_0 + \eta)^2 - \frac{1}{3}\rho h_0^3 w_{xt} \end{aligned}$$

4.4 Energy

The differential balance equation for the energy is obtained in a similar way, but is a bit more complicated. And there is actually different ways to describe this, depending on where the potential energy is defined to be zero. One form is found in [1] and one in [2]. Since the form used in [2] satisfies the Hamiltonian function corresponding to the KB system (3.15), and hence is exactly conserved, we use that one. The energy, sum of kinetic and potential energy, contained inside the given volume is then given by

$$\mathcal{E} = \frac{1}{2}\int_{x_1}^{x_2}\int_{-h_0}^{\eta} \rho|\nabla\phi|^2 dz dx + \int_{x_1}^{x_2}\int_{0}^{\eta} \rho g z dz dx.$$

Conservation of energy is given by

$$\begin{aligned} &\frac{d}{dt}\int_{x_1}^{x_2}\int_{-h_0}^{\eta} \frac{\rho}{2}|\nabla\phi|^2 \, dz dx + \frac{d}{dt}\int_{x_1}^{x_2}\int_{0}^{\eta} \rho g z \, dz dx \\ &= \left[\int_{-h_0}^{\eta} \left\{\frac{\rho}{2}|\nabla\phi|^2 + \rho g z\right\}\phi_x \, dz + \int_{-h_0}^{\eta} \phi_x P \, dz\right]_{x_2}^{x_1}. \end{aligned}$$

Similarly as above, after a little computation the differential balance for energy is obtained, and can be written

$$\begin{aligned} &\tfrac{d}{d\tilde{t}}\textstyle\int_{x_1/l}^{x_2/l}\left(\frac{\alpha^2}{2}\tilde{\eta}^2 + \frac{\alpha^2}{2}(1+\alpha\tilde{\eta})\tilde{w}^2 + \frac{\alpha^2\beta}{3}\tilde{w}\tilde{w}_{\tilde{x}\tilde{x}} + \frac{\alpha^2\beta}{6}\tilde{w}_{\tilde{x}}^2\right)d\tilde{x} \\ &= \left[\tfrac{\alpha^3}{2}\tilde{w}^3 + \alpha^2\tilde{w}\tilde{\eta}(1+\alpha\tilde{\eta}) + \tfrac{\alpha^2\beta}{3}\tilde{\eta}\tilde{w}_{\tilde{x}\tilde{x}} - \tfrac{\alpha^2\beta}{3}\tilde{w}_{\tilde{x}\tilde{t}}\right] + O(\alpha^4, \alpha^3\beta, \alpha^2\beta^2). \end{aligned} \quad (4.7)$$

We write this as

$$\frac{\partial}{\partial\tilde{t}}\tilde{E}+\frac{\partial}{\partial\tilde{x}}\tilde{q}_E=O(\alpha^4,\alpha^3\beta,\alpha^2\beta^2), \tag{4.8}$$

with

$$\begin{aligned}\tilde{E}&=\frac{\alpha^2}{2}\tilde{\eta}^2+\frac{\alpha^2}{2}(1+\alpha\tilde{\eta})\tilde{w}^2+\frac{\alpha^2\beta}{3}\tilde{w}\tilde{w}_{\tilde{x}\tilde{x}}+\frac{\alpha^2\beta}{6}\tilde{w}_{\tilde{x}}^2,\\ \tilde{q}_E&=\frac{\alpha^3}{2}\tilde{w}^3+\alpha^2\tilde{w}\tilde{\eta}(1+\alpha\tilde{\eta})+\frac{\alpha^2\beta}{3}\tilde{\eta}\tilde{w}_{\tilde{x}\tilde{x}}-\frac{\alpha^2\beta}{3}\tilde{w}_{\tilde{x}\tilde{t}},\end{aligned}$$

and with the scalings $E=\rho h_0c_0^2\tilde{E}$ and $q_E=\rho h_0c_0^3\tilde{q}_E$, the dimensional forms are

$$\begin{aligned}E&=\rho\bigg(\frac{g}{2}\eta^2+\frac{1}{2}(h_0+\eta)w^2+\frac{h_0^3}{3}ww_{xx}+\frac{h_0^3}{6}w_x^2\bigg),\\ q_E&=\rho\bigg(\frac{h_0}{2}w^3+g\eta w(h_0+\eta)+\frac{gh_0^3}{3}\eta w_{xx}-\frac{h_0^3}{6}ww_{xt}\bigg).\end{aligned} \tag{4.9}$$

As referred to in [2], the Hamiltonian function corresponding to the KB system (3.15) is

$$H=\rho\int_{-\infty}^{\infty}\left(\frac{g}{2}\eta^2+\frac{1}{2}(h_0+\eta)w^2-\frac{h_0^3}{6}w_x^2\right)dx. \tag{4.10}$$

The last expression for the energy E in (4.9) satisfies the Hamiltonian function,

$$H=\int_{-\infty}^{\infty}E\;dx, \tag{4.11}$$

and is therefore conserved.

4.5 Momentum conservation investigation

To this point, the equations presented for mass and momentum are just the KB-form of the equations for general Boussinesq systems given in [1]. Investigating further the momentum balance (4.6), we insert the non-dimensional momentum density and flux given by (4.5) to see if this expression can be simplified. We have

$$\begin{aligned}\frac{\partial}{\partial\tilde{t}}\tilde{I}+\frac{\partial}{\partial\tilde{x}}\tilde{q}_I&=\alpha\tilde{w}_{\tilde{t}}+\alpha^2(\tilde{w}\tilde{\eta})_{\tilde{t}}+\frac{1}{3}\alpha\beta\tilde{w}_{\tilde{x}\tilde{x}\tilde{t}}\\ &\quad+\alpha\tilde{\eta}_{\tilde{x}}+2\alpha^2\tilde{w}\tilde{w}_{\tilde{x}}+\alpha^2\tilde{\eta}\tilde{\eta}_{\tilde{x}}-\frac{1}{3}\alpha\beta\tilde{w}_{\tilde{x}\tilde{x}\tilde{t}}.\end{aligned}$$

Now, the $\tilde{w}_{\tilde{x}\tilde{x}\tilde{t}}$-terms disappear right away, and we transform to dimensional variables by (3.7), and after a little sorting of terms, we get

$$\begin{aligned}\frac{\partial}{\partial\tilde{t}}\tilde{I}+\frac{\partial}{\partial\tilde{x}}\tilde{q}_I&=\frac{l}{gh_0}(w_t+g\eta_x+ww_x)\\ &\quad+\frac{l}{gh_0}(\frac{1}{h_0}(w\eta)_t+ww_x+\frac{g}{h_0}\eta\eta_x).\end{aligned}$$

The expression inside the first parentheses is simply the second of the Kaup-Boussinesq equations (3.15), and can be set to zero when terms of order $O(\alpha\beta,\beta^2)$

are ignored. Further, we observe that the $(w\eta)_t$-term is now the only t-derivative. Writing out this term and using both of the equations (3.15) to substitute for η_t and w_t, and sorting the resulting terms leads to the following

$$\begin{aligned}\frac{\partial}{\partial\tilde{t}}\tilde{I}+\frac{\partial}{\partial\tilde{x}}\tilde{q}_I &= \frac{l}{gh_0}(-\frac{1}{h_0}(w^2\eta)_x-\frac{1}{3}h_0^2ww_{xxx})\\ &= \frac{l}{gh_0}\Big[-\frac{1}{h_0}(w^2\eta)_x-\frac{1}{3}h_0^2ww_{xxx}(-\frac{1}{3}h_0^2w_xw_{xx}+\frac{1}{3}h_0^2w_xw_{xx})\Big]\\ &= \frac{l}{gh_0}\Big[-\frac{1}{h_0}(w^2\eta)_x-\frac{1}{3}h_0^2(ww_{xx})_x+\frac{1}{3}h_0^2(\frac{1}{2}w_x^2)_x\Big],\end{aligned}$$

where the last two relations are obtained by subtracting and adding one term, recognizing the two middle terms as the product rule and the last term as the chain rule. We now see that the terms on the right-hand side can be written as the x-derivative of a function, say F, so we can write

$$\frac{\partial}{\partial\tilde{t}}\tilde{I}+\frac{\partial}{\partial\tilde{x}}\tilde{q}_I=\frac{\partial}{\partial x}F.$$

Hence, the momentum balance equation can be written as a partial differential equation when terms of order $O(\alpha\beta,\beta^2)$ are ignored. In particular, for solutions (η,w) of (3.15) which are smooth and decay to 0 as $x\to\pm\infty$, we have

$$\begin{aligned}\frac{d}{dt}\int_{-\infty}^{\infty}I(\eta,w) &= \int_{-\infty}^{\infty}\frac{\partial}{\partial t}I(\eta,w)\\ &= \int_{-\infty}^{\infty}\frac{\partial}{\partial x}F(\eta,w)-\int_{-\infty}^{\infty}\frac{\partial}{\partial x}q_I(\eta,w)=0\end{aligned}\tag{4.12}$$

Thus, conservation of momentum is exactly satisfied for the Kaup-Boussinesq system.

Chapter 5

Investigations of Kaup-Boussinesq for internal waves

5.1 Motivation

In the derivation of the Kaup-Boussinesq system we assume small amplitude waves, or small amplitude compared to the wavelength. Still, we want to see if it works for larger amplitude waves, or at least how large of an amplitude we can have while still having a reasonably good approximation. The motivation for investigating this is that when assuming solitary waves, the KB system and the extended Korteweg-deVries equation, also known as the Gardner equation, basically have the same form. For large amplitude internal solitary waves, a phenomena of quite broad waves is observed as the amplitude increases. This phenomena is referred to in for example [16], [13], [6] and [11]. In [11] it is also shown that the Gardner equation gives a good approximation for large amplitude waves, and this equation is also investigated in [13]. With that in mind, we use Gardner for comparison with the Kaup-Boussinesq system.

5.2 Equations and geometrical setup

The Kaup-Boussinesq system (KB) for internal waves (3.20) is investigated, and we look at solitary wave solutions of the system

$$\begin{aligned} \eta_t + \alpha u_x + \epsilon^2(\delta u_{xxx} + \gamma(\eta u)_x) = 0, \\ u_t + \beta \eta_x + \epsilon^2 \gamma u u_x = 0, \end{aligned} \tag{5.1}$$

where the parameters α, β, δ and γ are given by

$$\alpha = \frac{h_1 h_2}{\rho_2 h_1 + \rho h_2}, \qquad \beta = g(\rho_1 - \rho_2),$$

$$\delta = \frac{1}{3}\frac{(h_1 h_2)^2(\rho_2 h_2 + \rho_1 h_1)}{(\rho_2 h_1 + \rho_1 h_2)^2}, \qquad \gamma = \frac{\rho_1 h_2^2 - \rho_2 h_1^2}{(\rho_2 h_1 + \rho_1 h_2)^2}.$$

The Gardner equation (3.21) has the form

$$\eta_t + c_0\eta_x + \alpha_1\eta\eta_x + \alpha_2\eta^2\eta_x + \beta_1\eta_{xxx} = 0. \tag{5.2}$$

Here, the parameters are

$$\begin{gathered} c_0^2 = \tfrac{gh_1h_2(\rho_1-\rho_2)}{\rho_2h_1+\rho_1h_2}, \quad \alpha_1 = \tfrac{3c_0}{2h_1h_2}\tfrac{\rho_1h_2^2-\rho_2h_1^2}{\rho_2h_1+\rho_1h_2}, \\ \alpha_2 = \tfrac{3c_0}{h_1^2h_2^2}\left[\tfrac{7}{8}(\tfrac{\rho_1h_2^2-\rho_2h_1^2}{\rho_2h_1+\rho_1h_2})^2 - \tfrac{\rho_2h_1^3+\rho_1h_2^3}{\rho_2h_1+\rho_1h_2}\right], \quad \beta = \tfrac{c_0h_1h_2}{6}\tfrac{\rho_1h_1+\rho_2h_2}{\rho_2h_1+\rho_1h_2} \end{gathered} \tag{5.3}$$

The geometrical setup for the problem is shown in figure 5.1.

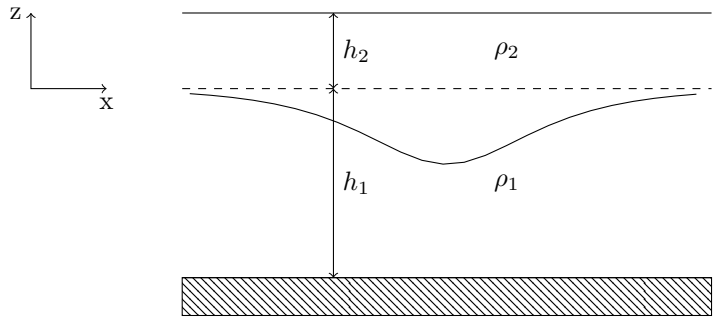

Figure 5.1: Geometric setup of the problem. It shows a typical solitary wave. The dashed line shows the equilibrium position. The motion in y-direction is ignored, so the motion is one-dimensional.

5.3 Discussion

We assume now that we have solitary waves, which means that the wave does not change its shape, and we can write the equations with respect to a new variable $\xi = x - ct$. Starting by putting $\eta(x,t) = \phi(x-ct)$ in the Gardner equation (5.2), and differentiate with respect to ξ, the following equation is obtained

$$-c\phi' + c_0\phi' + \frac{\alpha_1}{2}\phi\phi' + \frac{\alpha_2}{3}\phi^2\phi' + \beta_1\phi''' = 0, \tag{5.4}$$

where the derivatives are with respect to ξ. We now put $u(x,t) = \phi(x-ct)$ and $\eta(x,t) = \chi(x-ct)$, and substitute this into the KB system (5.1). In addition we put $\epsilon = 1$ to get a simpler calculation, which we can easily do without loss of generality, as stated in Chapter 3. Then the following system is obtained

$$\begin{cases} -c\chi' = -\alpha\phi' - \delta\phi''' - \gamma(\chi\phi)' \\ -c\phi' = -\beta\chi' - \frac{1}{2}\gamma(\phi^2)'. \end{cases} \tag{5.5}$$

From the second of these equations, we find an expression for χ and χ' given by ϕ and ϕ', put it into the first equation, and obtain

$$-(c^2 - \alpha\beta)\phi' + 3c\gamma\phi\phi' - \frac{3}{2}\gamma^2\phi^2\phi' + \delta\beta\phi''' = 0. \tag{5.6}$$

Taking a closer look at the two equations (5.4) and (5.6), we see that we have exactly the same terms. The only difference is the different parameters involved. To get the parameter values we set $h_1 = 3h_2$ or $h_1 = 4.13h_2$ in the upcoming calculations. The first case is from Guyenne [11] and the second from Grue [10], and we set $\rho_2 = 0.997\rho_1$. We also take into account that for KB $c^2 > \alpha\beta$, and for Gardner c is in the interval $0 < c < c_0 - \frac{\alpha_1^2}{6\alpha_2}$. The reason for this will be explained in a moment. With these values α, β and δ are positive while γ, α_1 and α_2 are negative. Comparing the two equations

$$\begin{aligned} -(c-c_0)\phi' + \frac{\alpha_1}{2}\phi\phi' + \frac{\alpha_2}{3}\phi^2\phi' + \beta_1\phi''' = 0, \\ -(c^2-\alpha\beta)\phi' + 3c\gamma\phi\phi' - \frac{3}{2}\gamma^2\phi^2\phi' + \delta\beta\phi''' = 0, \end{aligned} \tag{5.7}$$

we see that all the terms have the same signs. The only difference worth mentioning is that for the KB-system the wave speed c is involved in two terms, while for Gardner c is found only in the ϕ'-term.

A discussion of the derivative, as was done for the non-dimensional Gardner equation in [13], can be useful to find out where solitary waves can exist. We first integrate the dimensional Gardner equation (5.4) once, multiply it by ϕ' and then integrate once more. That yields

$$(\phi')^2 = \frac{c-c_0}{\beta_1}\phi^2 - \frac{1}{3}\frac{\alpha_1}{\beta_1}\phi^3 - \frac{\alpha_2}{6\beta_1}\phi^4, \tag{5.8}$$

Having a solitary wave solution, this has a maximum or a minimum. It also decays to zero as $x \to \pm\infty$. Hence, we can choose x big enough so that the quadratic term is much bigger than the cubic and quartic terms. Since α_1 and α_2 are negative while β_1 is positive, this means that $c > c_0$ must be satisfied for the quadratic term to be positive. If $c < c_0$, we could always have a point x big enough so that the quadratic term makes the expression on the right-hand side negative, which is not possible. This means that there can only be solitary wave solutions if $c > c_0$. We also know that this has to be negative solitary waves, since assuming a minimum $\phi(x_{min}) = \phi_{min}$, where the derivative is zero, we get

$$\frac{1}{\beta_1}\phi_{min}^2\left(c - c_0 - \frac{1}{3}\alpha_1\phi_{min} - \frac{1}{6}\alpha_2\phi_{min}^2\right) = 0.$$

Since $\phi_{min} = 0$ only gives the trivial solution $\phi = 0$, we must have

$$c - c_0 = \frac{1}{3}\alpha_1\phi_{min} + \frac{1}{6}\alpha_2\phi_{min}^2. \tag{5.9}$$

Here, since α_1 and α_2 are negative, ϕ_{min} must be negative. Assuming positive waves and a maximum here gives a contradiction. Solving this second order equation for the minimum gives

$$\phi_{min} = -\frac{\alpha_1}{\alpha_2} \pm \frac{1}{\alpha_2}\sqrt{\alpha_1^2 + 6\alpha_2(c-c_0)},$$

which again demands that

$$c \leqslant c_0 - \frac{\alpha_1^2}{6\alpha_2}, \tag{5.10}$$

not to take the square root of a negative number and get complex solutions. For solitary wave solutions to exist, this must be satisfied.

The corresponding equation for the derivative of KB (5.6) is

$$(\phi')^2 = \frac{c^2 - \alpha\beta}{\beta\delta}\phi^2 - c\frac{\gamma}{\beta\delta}\phi^3 + \frac{1}{4}\frac{\gamma^2}{\beta\delta}\phi^4. \tag{5.11}$$

A similar argument can be made here; a solitary wave solution having a maximum or a minimum and decaying to zero as $x \to \pm\infty$, choosing x big enough so that the quadratic is much bigger than the cubic and quartic terms. Observing that $c^2 > \alpha\beta$ for the quadratic term to be positive, so c must be in the interval $-\sqrt{\alpha\beta} < c < \sqrt{\alpha\beta}$. With similar argumentation as above, we find that for c in the negative interval we have positive solitary wave solutions and we have negative solutions in the positive interval. The waves will travel in opposite directions. Taking c positive gives negative solitary waves. This is because, assuming a minimum $\phi(x_{min}) = \phi_{min}$ and putting the derivative equal to zero, we get a similar equation to (5.9)

$$c^2 - \alpha\beta = c\gamma\phi_{min} - \frac{1}{4}\gamma^2\phi_{min}^2.$$

Knowing that γ is negative, ϕ_{min} must be negative for the right-hand side to be positive. Hence, we have negative solitary waves. Similarly, solving this second order equation simply gives

$$\phi_{min} = \frac{2}{\gamma}\Big(c \pm \sqrt{\alpha\beta}\Big),$$

which gives no further restrictions on c. For negative c, the same discussion would have been opposite but symmetric.

5.3.1 Phase plane diagrams

Integrating the equations (5.7) once, and introducing $\psi = \phi'$, the following system is obtained

$$\begin{aligned} \phi' &= \psi, \\ \psi' &= \frac{c - c_0}{\beta_1}\phi - \frac{\alpha_1}{2\beta_1}\phi^2 - \frac{\alpha_2}{3\beta_1}\phi^3 \end{aligned} \tag{5.12}$$

for the Gardner equation, and

$$\begin{aligned} \phi' &= \psi, \\ \psi' &= \frac{3}{\beta\delta}(c^2 - \alpha\beta)\phi - \frac{3}{2}\frac{c\gamma}{\beta\delta}\phi^2 - \frac{3}{2}\frac{\gamma^2}{\beta\delta}\phi^3 \end{aligned} \tag{5.13}$$

for KB. Before making phase plane diagrams, we find the critical points of the systems. For Gardner, we get

$$\begin{aligned} \phi' = 0 \quad &\Rightarrow \quad \psi = 0, \\ \psi' = 0 \quad &\Rightarrow \quad \phi\Big(\frac{c - c_0}{\beta_1} - \frac{\alpha_1}{2\beta_1}\phi - \frac{\alpha_2}{3\beta_1}\phi^2\Big) = 0. \end{aligned}$$

The last relation gives three solutions for ϕ

$$\phi = 0 \quad \text{and} \quad \phi = -\frac{3}{4}\frac{\alpha_1}{\alpha_2}\Big(1 \pm \sqrt{1 + \frac{16}{3}\frac{\alpha_2}{\alpha_1^2}(c - c_0)}\Big)$$

This means that we have the three critical points where ψ is zero for all three values of ϕ given above. Letting c go to the critical value $c \to c_0$ inside the square root gives a duplication of $\phi = 0$ and the negative $\phi = -\frac{3}{2}\frac{\alpha_1}{\alpha_2}$. The other critical value $c \to c_0 - \frac{\alpha_1^2}{6\alpha_2}$ gives the two solutions

$$\phi = -\frac{\alpha_1}{\alpha_2} \quad \text{and} \quad \phi = -\frac{1}{2}\frac{\alpha_1}{\alpha_2},$$

which are both negative.

Correspondingly, for KB we get

$$\begin{aligned} \phi' = 0 \quad &\Rightarrow \quad \psi = 0, \\ \psi' = 0 \quad &\Rightarrow \quad \phi = 0, \quad \phi = -\frac{1}{2}\frac{c}{\gamma}\Big(1 \pm \sqrt{9 - 8\frac{\alpha\beta}{c^2}}\Big). \end{aligned}$$

Knowing that $c > \sqrt{\alpha\beta}$ and letting c go to the critical value $c \to \sqrt{\alpha\beta}$ inside the square root, we get

$$\phi = 0 \quad \text{and} \quad \phi = -\frac{c}{\gamma}.$$

For $c > \sqrt{\alpha\beta}$ though, we get one positive and one negative solution for $\psi' = 0$. As c increases these two points will also get further and further away from the origin in both directions. This means that we get one critical point on the positive side of the ϕ-axis and one on the negative side, in addition to the one at the origin. For Gardner, both nonzero critical points will be on the negative side of the ϕ-axis, which will be clear when we draw the phase planes.

We now use the systems (5.12) and (5.13) to make phase plane diagrams for Gardner and KB with the help of a phase plane Matlab code made by John C. Polking at Rice University [17]. The parameter values are obtained using $h_2 = h_1/3 = 0.15$ and $\rho_2 = 0.997\rho_1 = 997$, which are consistent with the values used for the plots in the next section. Phase planes for KB and Gardner are made for a particle choice of c, and this is shown in Figure 5.2. We can see that we have one saddle point at the origin and one center on the negative ϕ-axis for both systems. The third critical point is also a saddle point for Gardner. For KB the third one is a center far from the origin on the positive ϕ-axis. A homoclinic orbit, marked in red, corresponding to solitary wave solutions is shown for both KB and Gardner in the phase planes. The KB diagram is zoomed in near the origin in Figure 5.3.

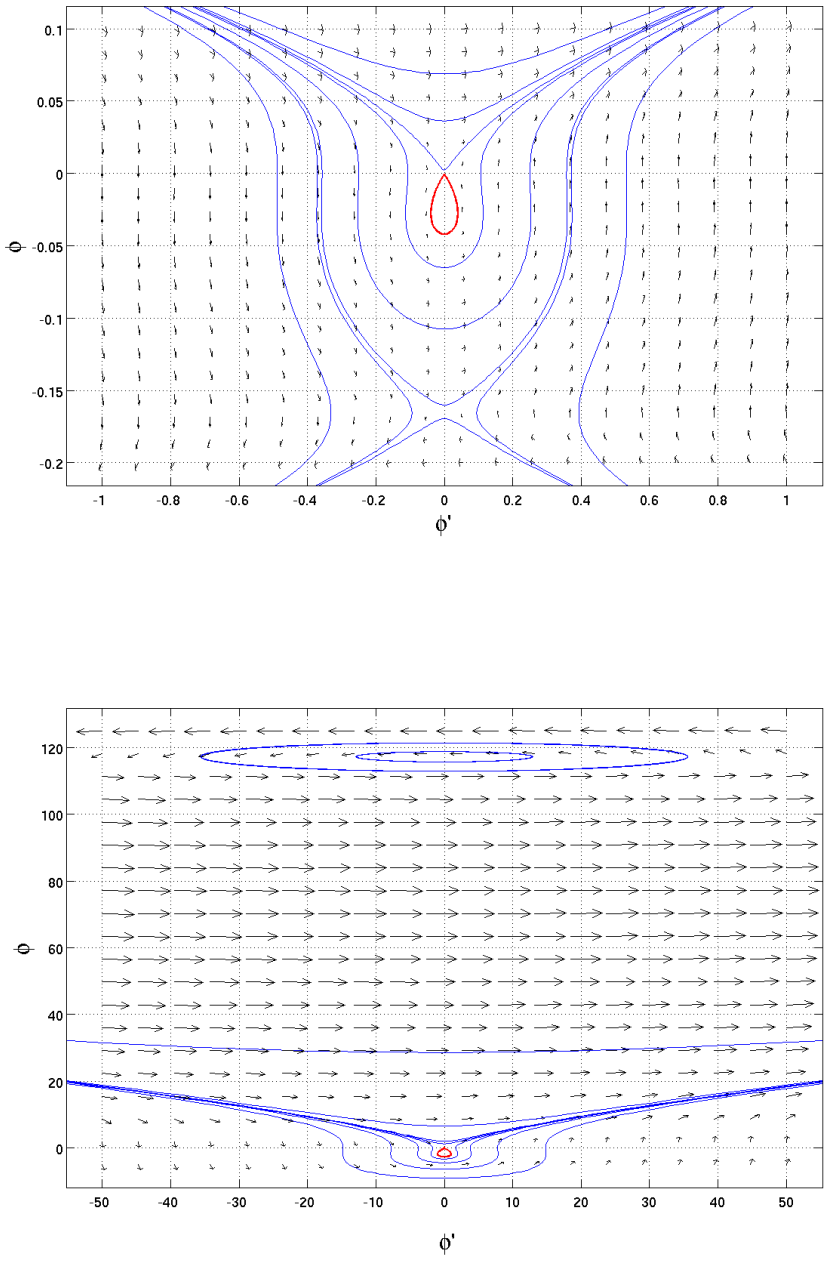

Figure 5.2: Phase plane diagram for Gardner (the upper one) and Kaup-Boussinesq.

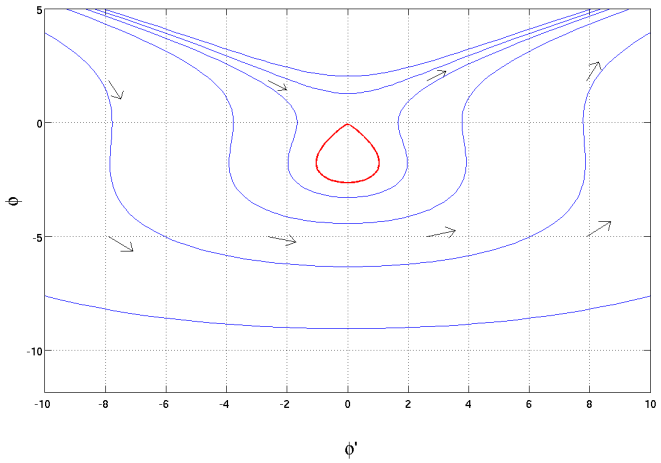

Figure 5.3: Phase plane diagram for KB, the lower part zoomed in.

We make a new phase plane diagram for Gardner, where c is close to the critical value given by (5.10), to see what happens then. From Figure 5.4 we see that the homo-clinic orbit goes from the origin almost down to the lower saddle point, and then back to the origin. When one puts c equal to the critical value, we see from Figure 5.5 that a solution goes exactly from the higher to the lower saddle point, and a solution going back. It seems like the closer c is to the critical value, the closer ϕ gets to the lower critical point before it returns to zero. Since c has no upper limit for KB, there is no corresponding phenomena to be observed.

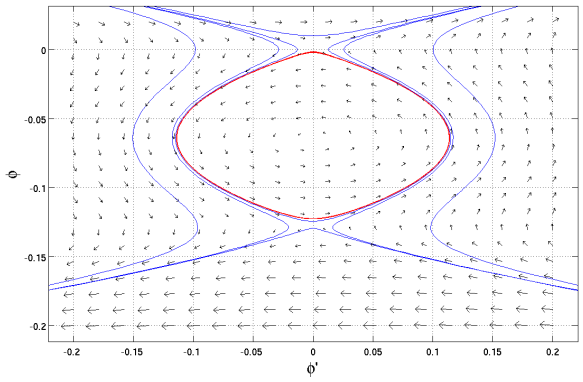

Figure 5.4: Phase plane diagram for Gardner with c near the critical value.

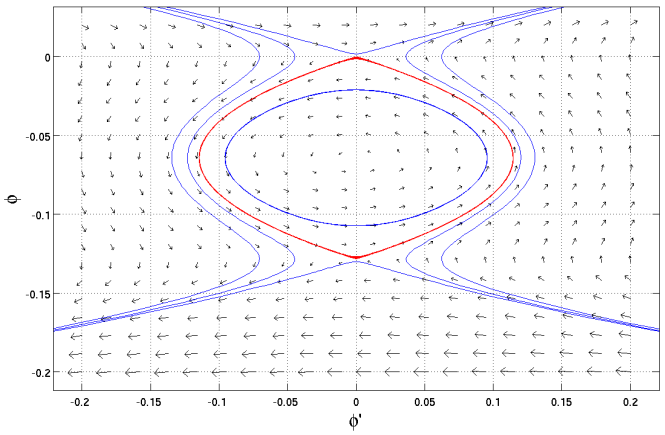

Figure 5.5: Phase plane diagram for Gardner with c equal to the critical value.

5.4 Solutions of Kaup-Boussinesq and Gardner

To investigate how good of an approximation the Kaup-Boussinesq system gives us, the solution of the system found by Guyenne [11] is used. If we use the form (5.5) of KB, it is easy to check that the solution by Guyenne

$$\begin{cases} \eta(x,t) = \frac{c}{\beta}u(x,t) - \frac{\gamma}{2\beta}u(x,t)^2 \\ \\ u(x,t) = 2\frac{\sqrt{\alpha\beta}}{\gamma}\frac{(\frac{c^2}{\alpha\beta}-1)}{cosh(\sqrt{\frac{\alpha}{\delta}(\frac{c^2}{\alpha\beta}-1)}(x-ct))+\frac{c}{\sqrt{\alpha\beta}}} \end{cases} \tag{5.14}$$

is actually a solution of this system of equations. The mathematical software Maple is used to check that (5.14) does indeed satisfy the system (5.1). Guyenne used this solution as an initial guess for the iterative procedure in solving the Hamiltonian system derived by Craig, Guyenne and Kalisch [8], and got results that matched experimental results and the nonlinear model of Grue et al. [10] pretty well.

For comparison of the solution (5.14) we mainly use the solution of the Gardner equation, but also results from the nonlinear model of Grue et al. [10] for the wave width and wave speed plots. The solution of the Gardner equation (5.2) used here is found in [11], and is of the form

$$\eta(x,t) = -\frac{\alpha_1}{\alpha_2}\frac{\nu}{2}\left[tanh(\frac{x-ct}{\Delta}+\delta) - tanh(\frac{x-ct}{\Delta}-\delta)\right] \tag{5.15}$$

where

$$\alpha_1 = \frac{3c_0(h_2-h_1)}{2h_1h_2},\ \alpha_2 = \frac{3c_0}{h_1^2h_2^2}\left[\frac{7}{8}(h_1-h_2)^2 - \frac{h_1^3+h_2^3}{h_1+h_2}\right]$$

$$\Delta^2 = -\frac{24\alpha_2\beta}{\alpha_1^2\nu^2},\ c_0^2 = \frac{gh_1h_2(\rho_1-\rho_2)}{\rho_1(h_1+h_2)},$$

$$\beta_1 = \frac{c_0h_1h_2}{6},\ \delta = \frac{1}{4}ln(\frac{1+\nu}{1-\nu}),\ c = c_0 - \frac{\alpha_1^2\nu^2}{6\alpha_2}, \tag{5.16}$$

where ν is a nonlinearity parameter, and lies in the interval $0 < \nu < 1$. We see here that for the parameters $\alpha_1,\ \alpha_2,\ \beta_1$ and c_0, the approximation $\rho_1 \approx \rho_2$ is used when compared with (5.3). This is done except for the numerator in c_0, because it here would make $c_0 = 0$. Grue's results were obtained from the graphs in [10] and [11], and there it is shown that for big amplitudes we get broader solitary wave solutions. This phenomena is also referred to in [13]. The closer the amplitude is to the height of the top layer, that is the closer the relationship η/h_2 gets to 1, the broader the solitary wave solutions are. We therefore expect the solutions to get broader as the amplitude increases.

5.5 Results

To show how the Kaup-Boussinesq model works, we plot the wave profile for different amplitudes and compare it with the solution of the Gardner equation (5.15). We also plot the wave width at various amplitudes, and finally a plot showing how the wave speed varies with increasing amplitude. These plots should give us a good insight to how well the Kaup-Boussinesq system models internal waves.

5.5.1 Wave profiles

Figure 5.6 shows the solutions (5.14) and (5.15) at different amplitudes. To get these amplitudes the wave speed c is varied, and for KB we can see from the solution that c is restricted by $c > \sqrt{\alpha\beta}$. To get the plots for the Gardner equation, we observe from (5.16) that c is dependent on the nonlinearity parameter ν, so this is varied between $0 < \nu < 1$. These plots show us that for small amplitudes the solution of KB fits quite well with the Gardner solution, but for bigger amplitudes we clearly see that the resulting wave profiles are not broad enough. We see that the Gardner equation, which gives a good approximation, gives broader wave profiles for bigger amplitudes. A plot of Gardner near the critical value $c = c_0 - \frac{\alpha_1^2}{6\alpha_2}$ corresponding to $\nu \to 1$ is also done. This wave profile is shown in Figure 5.7.

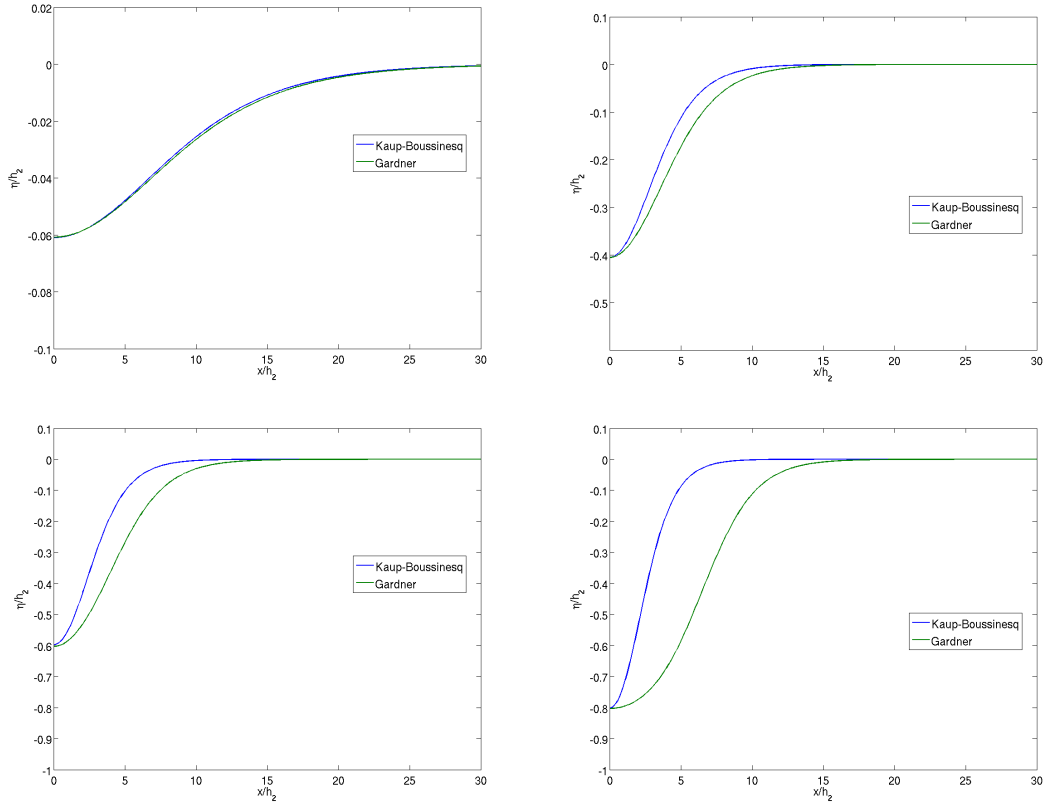

Figure 5.6: Comparison of wave profiles of the Kaup-Boussinesq model and the Gardner equation.

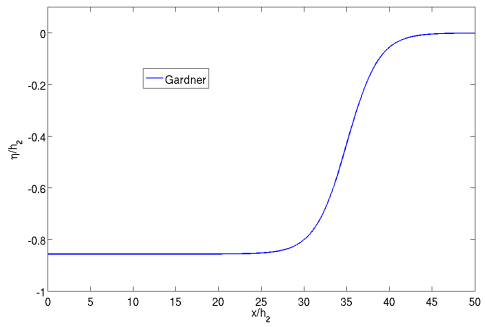

Figure 5.7: A plot of the waveprofile for Gardner with c near the critical value. Here $\nu = 0.9999999999999999$.

5.5.2 Width comparison

Figure 5.8, on the other hand, shows a comparison of solitary wave widths for the Kaup-Boussinesq model, the Gardner equation and the fully nonlinear

model of Grue et al. In figure 5.8 a) we have $h_1 = 3h_2$, and it is clear from Gardner and Grue et al. that for small amplitudes we have broad solitary wave solutions. For bigger amplitudes we get narrower waves, and the closer η/h_2 gets to 1, the broader the waves become again. From the figure we see that the Kaup-Boussinesq solution gets narrower the bigger the amplitude gets, but the tendency of broader waves for increasing amplitude does not show. In figure 5.8 b) we have $h_1 = 4.13h_2$. Here, the broadening is not so clear, but it can still be observed. It seems like the broadening of the waves for bigger amplitudes depends on the relationship h_1/h_2, but from both figures we see that the Kaup-Boussinesq equation does not give a satisfactory approximation.

a)

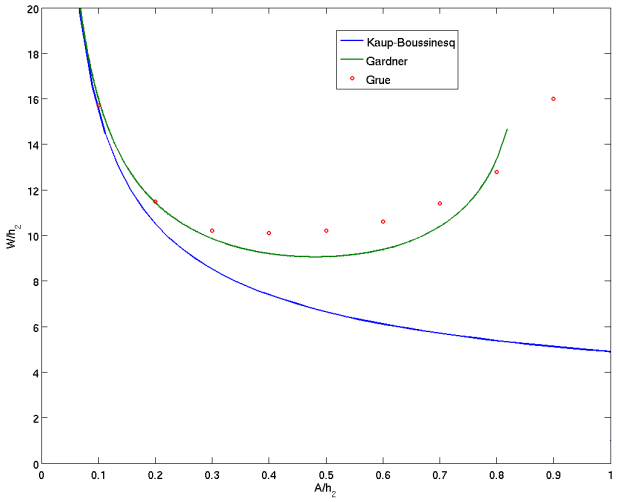

b)

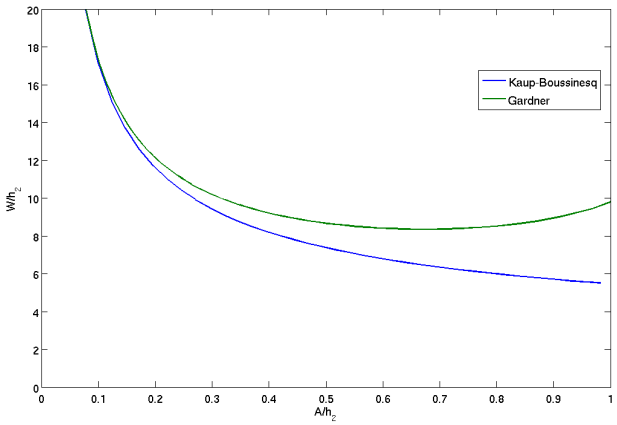

Figure 5.8: Comparison of solitary wave widths for the Kaup-Boussinesq model, the Gardner equation and the fully nonlinear model of Grue et al. In figure a) we have $h_1 = 3h_2$ and in figure b) $h_1 = 4.13h_2$.

5.5.3 Speed comparison

Figure 5.9 shows that for increasing amplitude the wave speed seems to stabilize for the model of Grue et al. and for the Gardner equation, while we for KB get increasing wave speed as the amplitude increases. This again show deviating results from Grue et al. and Gardner. We can easily see this from the solution (5.14). The amplitude continues to increase with increasing c, since there is no upper limit for c.

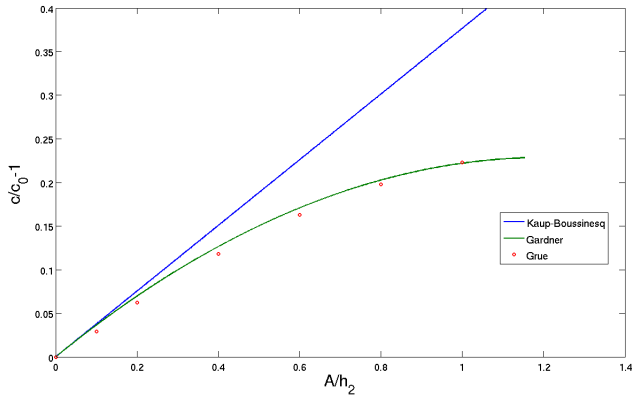

Figure 5.9: A plot of the wave speed c relative to amplitude for the Kaup-Boussinesq model, the Gardner equation and the fully nonlinear model of Grue et al. We have $h_1 = 4.13h_2$.

5.6 Conclusion

All the figures point towards the same conclusion, that the Kaup Boussinesq model is not really a good choice to describe internal solitary waves, as long as we are modeling large-amplitude waves. This, even though Gardner and KB have the same form. It seems like the upper limit for c in the Gardner equation, in addition to the locations of the critical points in the phase plane, are the reasons why Gardner models large amplitude internal solitary waves better than Kaup-Boussinesq does. For Gardner, the two non-zero critical points became closer to each other for increasing c. This "forced" the solution ϕ to spend more time in the lower part of the phase plane, creating the broad waves, until it reached the maximum c. For Kaup-Boussinesq, the two non-zero critical points just became more apart for increasing c, which only resulted in narrower waves.

Chapter 6

Numerical Method

The objective of this chapter is to introduce the principle of spectral methods as a numerical tool to solve equations, both ordinary differential equations (ODEs) and partial differential equations (PDEs). In particular we will look at the Fourier collocation method with a pseudospectral transform method to compute nonlinear terms in an efficient way. This provides the foundation for the numerical work presented in the next chapter. The theory here is based on the book of Spectral Methods in Fluid Dynamics [5].

6.1 Spectral Methods

Spectral methods are used to solve certain differential equations. The way this is done is to write the solution as an expansion, for example a Fourier series, and find the coefficients of the series. If we have a differential equation, where u is the dependent variable, the approximate solution is represented as

$$u(x,t) = \sum_{k=-\infty}^{\infty} \hat{u}_k(t)\phi_k(x). \tag{6.1}$$

Here ϕ_k are called trial functions and $\hat{u}_k$ the expansion coefficients. The trial functions here are infinitely differentiable global functions. When using the Fourier approach the trial functions are trigonometric polynomials $\phi_k(x) = e^{ikx}$, but Chebyshev and Legendre polynomials are also frequently used.

In general, the approximation (6.1), is calculated up to N terms

$$u^N(x,t) = \sum_{k=-N/2}^{N/2-1} \hat{u}_k(t)\phi_k(x). \tag{6.2}$$

The reason for the $N/2$-degree approximation is because of the way spectral methods are implemented, so this is the approximation we use later on. This does, in general, not alone satisfy the differential equation. In addition, test functions are used to ensure that the problem is satisfied by minimizing the error produced by the approximate series (6.2). If we have the problem

$$\frac{\partial u}{\partial t} = M(u),$$

where $M(u)$ contains spatial derivatives, then the test functions $\psi_k(x)$ satisfy

$$\int_0^{2\pi} \left[\frac{\partial u^N}{\partial t} - M(u^N) \right] \psi_k(x) \, dx = 0, \tag{6.3}$$

for $k = -N/2, ..., N/2 - 1$. There is three common spectral methods that differ from each other by the choice of these test functions. The Galerkin, tau and collocation methods. Essentially the Galerkin and tau approach are implemented in terms of the expansion coefficients, while the collocation method uses the value of the unknown function in certain physical points. The Galerkin and tau methods are difficult and impractical to apply to nonlinear problems, while the spectral collocation approach is more attractive. Therefore, the collocation approach is used in this thesis. For the collocation method, the test functions are

$$\psi_j(x) = \delta(x - x_j), \quad j = 1, ..., N - 1,$$

and x_j are the grid points for the method. Then (6.3) reduces to

$$\frac{\partial u^N}{\partial t} - M(u^N)\Big|_{x=x_j} = 0, \quad j = 1, ..., N - 1.$$

That means, the approximation (6.2) must satisfy the differential equation at each grid point.

If we require the sequence $\{\phi_k\}$ to be orthogonal, we get a linear transformation between u and the expansion coefficients $\{\hat{u}_k(t)\}$, a transform between the physical space and transform space. This transform is invertible if the system is complete in a Hilbert space. This means that we can go from physical space to transform space, and functions can be described in both spaces. Since the expansion coefficients in (6.2) in general depends on all the values of the function, we use a discrete transform and approximate the expansion coefficients using only a finite number of points. This can be done if the spectral accuracy is retained when replacing the finite transform with the discrete one. The Fourier system is an orthogonal system which guarantee spectral accuracy, so we can use Fourier transformation. Hence, we introduce first the Fourier transform. Further, we discuss the errors using the Fourier approach, and how to differentiate using the approximation, since we are solving differential equations. Then we move on to how nonlinear terms are treated with a pseudospectral approach.

6.1.1 Fourier Theory

The general approximation in the Fourier sense of a function u is defined as

$$Su = \sum_{k=-\infty}^{\infty} \hat{u}_k e^{ikx}.$$

This we call the Fourier series of the function. Here, e^{ikx} is orthogonal on the interval $(0, 2\pi)$, and the Fourier coefficients satisfy

$$\hat{u}_k = \frac{1}{2\pi} \int_0^{2\pi} u(x) e^{-ikx} dx \quad k = 0, \pm 1, \pm 2, ... \tag{6.4}$$

This is known as the continuous Fourier transformation. The function u is now approximated by the trigonometric polynomials

$$P_N u(x) = \sum_{k=-N/2}^{N/2-1} \hat{u}_k e^{ikx}.$$

Often the Fourier coefficients (6.4) are not known in this closed form, and we got a problem with recovering the information about the function calculated in the transform space, so the coefficients must be approximated in some way. Thus, we introduce the discrete Fourier transform (DFT) and the discrete Fourier coefficients. Considering now the grid points

$$x_j = \frac{2\pi j}{N} \quad j = 0, ..., N-1 \tag{6.5}$$

in physical space. The discrete Fourier coefficients of the function u are defined as

$$\tilde{u}_k = \frac{1}{N} \sum_{j=0}^{N-1} u(x_j) e^{-ikx_j} \quad -\frac{N}{2} \leqslant k \leqslant \frac{N}{2} - 1. \tag{6.6}$$

The function is defined on the interval $(0, 2\pi)$, and with the help of the orthogonality relation

$$\frac{1}{N} \sum_{j=0}^{N-1} e^{ipx_j} = \begin{cases} 1 & \text{if } p = Nm, \ m = 0, \pm 1, \pm 2, ... \\ 0 & \text{otherwise} \end{cases} \tag{6.7}$$

we have an inversion formula for recovering the physical points

$$u(x_j) = \sum_{k=-N/2}^{N/2-1} \tilde{u}_k e^{ikx_j} \quad j = 0, ..., N-1. \tag{6.8}$$

This is referred to as the inverse discrete Fourier transformation. The discrete Fourier approximation of u is then

$$u(x) \approx I_N u(x) = \sum_{k=-N/2}^{N/2-1} \tilde{u}_k e^{ikx}, \tag{6.9}$$

Here, I stands for trigonometric interpolant, since we only use a finite number of points to approximate the function. The computations of the DFT (6.6) and the inverse DFT (6.8) can be accomplished by the Fast Fourier Transformation algorithm (FFT), which requires $O(N \log_2 N)$ operations.

6.1.2 Aliasing error for DFT

When we use the Fourier approach there is a truncation error associated with the approximation, since we only have an N-terms expansion. This is given by for example the L^2-norm

$$||u - P_N u||_{L^2}$$

for the continuous Fourier transformation, and

$$||u - I_N u||_{L^2}$$

for the discrete one. The discrete Fourier coefficients (6.6) can be seen as an approximation of the exact continuous Fourier coefficients (6.4) using the trapezoidal rule to evaluate the integral, and thus we get an extra error when using the DFT instead of the continuous transformation. We have the following relation between the coefficients

$$\tilde{u}_k = \hat{u}_k + \sum_{\substack{m=-\infty \\ m\neq 0}}^{\infty} \hat{u}_{k+Nm}, \qquad k = -N/2, ..., N/2 - 1.$$

We get an error because the $(k + Nm)^{th}$ frequency "aliases" the k^{th} frequency on our grid. This is because of the fact that $e^{ikx_j} = e^{i(k+Nm)x_j}$, so that they are not possible to distinguish from each other at the points x_j. Another way to write this is

$$I_N u = P_N u + R_N u,$$

where

$$R_N u = \sum_{k=-N/2}^{N/2-1} \left(\sum_{\substack{m=-\infty \\ m\neq 0}}^{\infty} \hat{u}_{k+Nm} \right) e^{ikx}.$$

This $R_N u$ is called the "aliasing" error. It has been proven though, that this error is asymptotically of the same order as the truncation error. This means that using DFT does not lead to any new difficulties concerning errors, at least not for linear terms. Aliasing errors due to nonlinear terms are discussed in the next section.

6.1.3 Differentiation

Working with spectral methods, differentiation depends on whether we are in physical or transform space. Differentiation in the transform space is done easily by multiplying each coefficient with ik. Hence, using DFT we simply multiply the coefficients in (6.6) by ik, and then transform back to (6.8). Thus, the derivative is based on the values of u at the grid points (6.5). The resulting derivative $D_N u$, is called the Fourier collocation derivative and is given by

$$D_N u = \sum_{k=-N/2}^{N/2-1} a_k e^{ikx},$$

where

$$a_k = \frac{ik}{N} \sum_{j=0}^{N-1} u_j e^{-ik\frac{2\pi j}{N}}.$$

Since this derivative is only based on the values at the grid points, it is the grid values of the derivative of the DFT, so we have

$$D_N u = (I_N u)',$$

and in general we have

$$D_N u \neq I_N u',$$

which is the interpolation of the derivative, so interpolation and differentiation do not commute. For the continuous transform however, truncation and differentiation commute, $(P_N u)' = P_N(u')$. That being said, collocation differentiation is spectrally accurate because the error and the truncation error of the derivative $P_N u'$ are of the same order, so one can safely use the collocation derivative in spectral methods.

6.1.4 Pseudospectral transform method

With the nonlinear terms a direct multiplication in the Fourier space is expensive, but with the use of transform methods they can be evaluated in less operations. The pseudospectral approach involves a multiplication in the physical space rather than the Fourier space, and then a transformation back to the Fourier space. When this is done, we get an aliasing error. The occurring error is explained here. If we look at a general quadratic term

$$w(x) = u(x)v(x), \tag{6.10}$$

with an infinite series expansion, the convolution sum will be

$$\hat{w}_k = \sum_{m+n=k} \hat{u}_m \hat{v}_n. \tag{6.11}$$

When u, v and w are approximated with the N degree continuous Fourier series, we have

$$\hat{w}_k = \sum_{\substack{m+n=k \\ |m|,|n| \leqslant N/2}} \hat{u}_m \hat{v}_n, \tag{6.12}$$

where $|k| \leqslant N/2$. Here

$$u(x) = \sum_{m=-N/2}^{N/2-1} \hat{u}_m e^{imx}$$

$$v(x) = \sum_{n=-N/2}^{N/2-1} \hat{u}_n e^{inx}$$

$$\hat{w}_k = \frac{1}{2\pi} \int_0^{2\pi} w(x) e^{-ikx} dx.$$

The summation (6.12) takes $O(N^2)$ operations, which is much too expensive. The use of transform methods reduces this to $O(N \log_2 N)$ operations.

The product we want to achieve (6.12), and the pseudospectral approach for evaluating this is based on using the inverse discrete Fourier transformation (DFT) to transform $\hat{u}_m$ and $\hat{v}_n$ back to the original spatial picture, carry out the multiplication similar to (6.10), and then transform back. We approximate

u, v and w with the DFT. We have

$$\begin{aligned} u(x_j) &= \textstyle\sum_{k=-N/2}^{N/2-1} \tilde{u}_k e^{ikx_j} \\ v(x_j) &= \textstyle\sum_{k=-N/2}^{N/2-1} \tilde{v}_k e^{ikx_j} \end{aligned} \qquad j = 0, 1, ..., N-1$$

and define

$$w(x_j) = u(x_j)v(x_j) \qquad j = 0, 1, ..., N-1.$$

We have

$$\tilde{w}_k = \frac{1}{N} \sum_{j=0}^{N-1} w(x_j) e^{-ikx_j}, \qquad k = -\frac{N}{2}, ..., \frac{N}{2} - 1$$

where the grid points are $x_j = 2\pi j/N$. This leads to

$$\tilde{w}_k = \sum_{m+n=k} \hat{u}_m \hat{v}_n + \sum_{m+n=k\pm N} \hat{u}_m \hat{v}_n$$

$$\tilde{w}_k = \hat{w}_k + \sum_{m+n=k\pm N} \hat{u}_m \hat{v}_n,$$

when we use the orthogonality relation (6.7). Comparing this to the convolution sum (6.12), we see that we have included an extra term using the DFT in the transformations back and forth, the aliasing error. This is why the method is called pseudospectral, because the product of two functions is not computed in the right way. The convenience of this however, is that taking the product in this way still takes $O(N\log_2 N)$ operations, and we can also use filter methods to remove the aliasing error.

6.2 Numerical procedure

The method used in the next chapter works as follows. We start off with a PDE, and use the Fourier collocation method to transform the PDE to an ODE in the Fourier-space, and use the Fourier collocation differentiation operator D from Section 6.1.3 for the spatial derivatives. We use the pseudospectral transform method for the nonlinear terms. They are computed in the physical space, so we transform back to the original spatial representation, carry out the multiplication, then transform back. For the transformations we use the Fast Fourier Transformation (fft in Matlab).

One usually use a condition where $\hat{u}_{-N/2}$ is set to zero. This is because we want $u^N(t)$ to be real-valued, and if $\hat{u}_{-N/2}$ has an imaginary part this will not be the case. This comes from the fact that k ranges from $-N/2$ to $N/2-1$ and not up to $N/2$, so $-N/2$ appears unsymmetrically.

The resulting equation is then usually discretized in time by an explicit method for the non-linear term and an implicit method for the linear ones, and here we use the implicit second order Crank-Nicolson method on the linear terms and the explicit second order Adams-Bashforth multistep method on the nonlinear terms. It is worth mentioning that the Crank-Nicolson method is maybe not

normally used on the type of problem considered here, because we in the next chapter see that the eigenvalues of our problem are imaginary, while the Crank-Nicolson method is A-stable for negative complex eigenvalues. We are therefore working at the boundary of the area of stability. However, since the resulting matrix of the problem is diagonal, the implicit Crank-Nicolson becomes explicit. These two methods are also used for a similar problem by Kalisch and Bona in [12], with good results. For the differential equation

$$y' = f(t, y),$$

the Adams-Bashforth formula is given by

$$y_{n+1} = y_n + \frac{3}{2}\Delta t f_n - \frac{1}{2}\Delta t f_{n-1},$$

and Crank-Nicolson by

$$y_{n+1} = y_n + \frac{\Delta t}{2}(f_n + f_{n+1}).$$

Since Adams-Bashforth is a multi-step method, the Euler method

$$y_{n+1} = y_n + \Delta t f_n$$

is used for the first time step on the nonlinear terms. At the end of the iterations, we use the inverse fast Fourier transform (ifft) to get back to the original spatial picture.

Chapter 7

Kaup-Boussinesq for surface waves: Numerical Results

In this chapter, we use the spectral collocation method for numerical approximation of solutions of the KB system. The KB-system is a complex system, in the sense that we have a coupled set of equations which are both nonlinear. In order to break down the problem, or to take it step by step so to say, we start off with the slightly easier KdV-equation. We start by looking at the linear part, then include the nonlinear part. Then we move on to the KB system, taking first the linear part of it into investigation before we at last work with the full KB-system. Doing things this way, we get to see that our method actually works on simpler problems than the KB system. Using the Fourier approach, we assume periodicity from 0 to 2π. We therefore use the scaling $x \to ax$, where $a = \frac{L}{2\pi}$. Then we have periodicity on the interval $[0, L]$. This means that $\frac{\partial}{\partial x} \to \frac{1}{a}\frac{\partial}{\partial x}$, so whenever we write $\frac{\partial}{\partial x}$ in the following, we mean $\frac{1}{a}\frac{\partial}{\partial x}$. Since this appears with every x-derivative, it is implemented in the code simply by letting $k \to \frac{k}{a}$.

7.1 The linear part of KdV

We start off by looking at the linear part of the KdV-equation, an easy, linear, uncoupled PDE. That is, an equation containing just a time derivative and a dispersive term

$$\eta_t + \eta_{xxx} = 0. \tag{7.1}$$

This equation is fairly easy to work with, and we also know the analytical solution

$$\eta(x,t) = \cos(\kappa x + \kappa^3 t). \tag{7.2}$$

Using the second order Crank-Nicolson for the time iterations, we get

$$\frac{\eta_{n+1} - \eta_n}{\Delta t} = -\frac{\partial_x^3 \eta_{n+1} + \partial_x^3 \eta_n}{2}.$$

Transforming to the Fourier space using the discrete Fourier transform (DFT) (6.6) from the previous chapter, we get

$$\hat{\eta}_{n+1} - \hat{\eta}_n = -\frac{\Delta t}{2}\Big((ik)^3\hat{\eta}_{n+1} + (ik)^3\hat{\eta}_n\Big).$$

Here the hats indicates that we are in the Fourier space. Sorting terms of n and $n+1$ gives

$$\hat{\eta}_{n+1} = \frac{1 + \frac{\Delta t}{2}ik^3}{1 - \frac{\Delta t}{2}ik^3}\hat{\eta}_n.$$

The computations are done with $N = 1024$ modes, and a domain of length $L = 100$. To check that the method works properly, a convergence analysis is done with comparison of the analytical and exact solution. Several different time steps are tested, the error and the ratio between the errors from time step to time step are calculated. With the initial condition

$$\eta = \cos(\frac{2\pi}{L}x),$$

time iteration up to $T = 10$, and comparison with the exact solution

$$\eta = \cos(\frac{2\pi}{L}x + T),$$

the results are shown in Table 7.1. We know that the local truncation error e for an iterative method of order p is

$$e \leqslant |f''(\xi)|(\Delta t)^p.$$

If we have an error e_1 for a time step Δt, and an error e_2 for a time step $\Delta t/2$, we get a ratio

$$\frac{e_1}{e_2} = \frac{(\Delta t)^p}{(\Delta t/2)^p} = 2^p.$$

For a second order method this ratio should be 4. Using time steps such that the next one is half of the previous one, calculating this ratio is therefore an easy way to check that the method works. We see from Table 7.1 that the method works for the equation (7.1). A plot of the wave profile for $dt = 0.1$ can be seen in Figure 7.1

dt	L^∞**-error**	**ratio**
0.1000	0.0083	
0.0500	0.0021	3.9955
0.0250	5.2078e-04	3.9989
0.0125	1.3021e-04	3.9997
0.0063	3.2552e-05	3.9999
0.0031	8.1380e-06	4.0000
0.0016	2.0345e-06	4.0000
7.8125e-04	5.0863e-07	4.0000
3.9063e-04	1.2716e-07	4.0000
1.9531e-04	3.1789e-08	4.0000

Table 7.1: Errors and ratio for different time steps of the linear part of the KdV equation. The next time step is half of the last one, for each test.

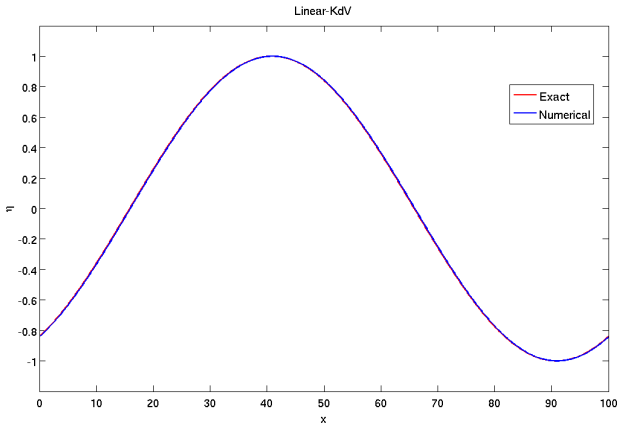

Figure 7.1: Wave profile of the linear part of the KdV equation for $dt = 0.1$.

7.2 The KdV equation

In the next step, we look at the KdV equation of the form

$$\eta_t + \eta_{xxx} + \eta\eta_x = 0. \tag{7.3}$$

Here, the only difference is the inclusion of the nonlinear term $\eta\eta_x$. This equation can also be written in the form

$$\eta_t + \eta_{xxx} + \frac{1}{2}(\eta^2)_x = 0.$$

In [15] it is stated that the solitary wave solution of this is of the form

$$12\kappa^2 \text{sech}^2(\kappa x).$$

Indeed

$$12\kappa^2 \text{sech}^2(\kappa(x - 4\kappa^2 t)),$$

satisfies (7.3), and this is used as an exact solution for time t in our code. In the same way as was done in the first section, we use the second order Crank-Nicolson on the linear part, and now we use the explicit Adams-Bashforth method on the nonlinear part. This leads to

$$\frac{\eta_{n+1} - \eta_n}{\Delta t} = -\frac{\partial_x^3\eta_{n+1} + \partial_x^3\eta_n}{2} - (\frac{3}{2}\frac{1}{2}\partial_x(\eta^2)_n - \frac{1}{2}\frac{1}{2}\partial_x(\eta^2)_{n-1}).$$

In the same way we transform to the Fourier space, and sort the terms, which gives us

$$\hat{\eta}_{n+1} = \frac{1 + \frac{\Delta t}{2}ik^3}{1 - \frac{\Delta t}{2}ik^3}\hat{\eta}_n + \frac{-\frac{3\Delta t}{4}ik}{1 - \frac{\Delta t}{2}ik^3}\hat{\eta^2}_n + \frac{\frac{\Delta t}{4}ik}{1 - \frac{\Delta t}{2}ik^3}\hat{\eta^2}_{n-1}.$$

Here, the nonlinear terms are calculated in the pseudospectral way. We use the same discretization and procedure, and the results for the errors obtained are

shown in Table 7.2. A plot of the wave profile for $dt = 0.1$ is shown in Figure 7.2.

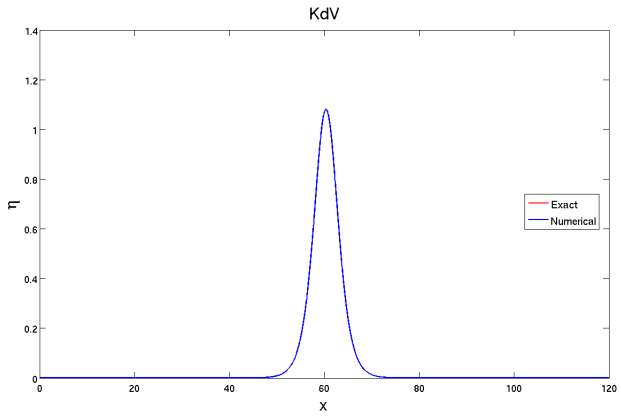

Figure 7.2: Wave profile of the KdV equation for $dt = 0.1$.

dt	L^∞**-error**	**ratio**
0.1000	4.9804e-04	
0.0500	1.2442e-04	4.0031
0.0250	3.1088e-05	4.0020
0.0125	7.7697e-06	4.0012
0.0063	1.9421e-06	4.0007
0.0031	4.8549e-07	4.0003
0.0016	1.2137e-07	4.0002
7.8125e-04	3.0341e-08	4.0001
3.9063e-04	7.5852e-09	4.0000
1.9531e-04	1.8963e-09	4.0000

Table 7.2: Errors and ratio for different time steps of the KdV equation. The next time step are half of the last one, for each test.

7.3 The linear part of Kaup

We now turn to the Kaup-Boussinesq system (3.15)

$$\eta_t = -w_x - \tfrac{1}{3}w_{xxx} - (\eta w)_x,$$

$$w_t = -\eta_x - \tfrac{1}{2}(w^2)_x.$$

To solve this system we first diagonalize it, and then transform it to Fourier space like we did for the KdV equation. To see that the method works also for this coupled system, we start with the linear part

$$\begin{aligned} \eta_t &= -w_x - \tfrac{1}{3}w_{xxx}, \\ w_t &= -\eta_x. \end{aligned} \tag{7.4}$$

This system has an exact solution of the form

$$\sin(\kappa x - \omega t).$$

Substituting this solution for w, we find ω and η

$$w(x,t) = \sin(\kappa x - \sqrt{1 - \tfrac{\kappa^2}{3}}t),$$

$$\eta(x,t) = \sqrt{1 - \tfrac{\kappa^2}{3}}\,\sin(\kappa x - \sqrt{1 - \tfrac{\kappa^2}{3}}t).$$

This exact solution is used to compare with the numerical solution, as initial condition we put $t = 0$ here. The system (7.4) can be written

$$\begin{bmatrix} \eta_t \\ w_t \end{bmatrix} = \begin{pmatrix} 0 & -\frac{\partial}{\partial x} - \frac{1}{3}\frac{\partial^3}{\partial x^3} \\ -\frac{\partial}{\partial x} & 0 \end{pmatrix} \begin{bmatrix} \eta \\ w \end{bmatrix}.$$

When transformed into the Fourier space, using DFT, we can write

$$\begin{bmatrix} \hat{\eta}_t \\ \hat{w}_t \end{bmatrix} = ik \begin{pmatrix} 0 & \frac{k^2}{3} - 1 \\ -1 & 0 \end{pmatrix} \begin{bmatrix} \hat{\eta} \\ \hat{w} \end{bmatrix}. \tag{7.5}$$

To diagonalize, we find the eigenvalues of the matrix and the corresponding eigenvectors to be

$$\lambda_{1,2} = \pm\sqrt{1 - \frac{k^2}{3}}, \quad \mathbf{a}_1 = \begin{bmatrix} \sqrt{1 - \frac{k^2}{3}} \\ 1 \end{bmatrix}, \quad \mathbf{a}_2 = \begin{bmatrix} -\sqrt{1 - \frac{k^2}{3}} \\ 1 \end{bmatrix}.$$

Now, using the relation

$$\begin{bmatrix} \hat{\eta} \\ \hat{w} \end{bmatrix} = \mathbf{T} \begin{bmatrix} \hat{x} \\ \hat{y} \end{bmatrix},$$

where $\mathbf{T}$ is the matrix with the eigenvectors as columns

$$\mathbf{T} = \begin{bmatrix} \sqrt{1 - \frac{k^2}{3}} & -\sqrt{1 - \frac{k^2}{3}} \\ 1 & 1 \end{bmatrix},$$

we obtain the new diagonalized system in new variables x and y

$$\begin{bmatrix} \hat{x}_t \\ \hat{y}_t \end{bmatrix} = ik \begin{pmatrix} \sqrt{1-\frac{k^2}{3}} & 0 \\ 0 & -\sqrt{1-\frac{k^2}{3}} \end{pmatrix} \begin{bmatrix} \hat{x} \\ \hat{y} \end{bmatrix}. \tag{7.6}$$

Here, we have used that

$$\mathbf{D} = \mathbf{T^{-1}AT},$$

where $\mathbf{D}$ is the diagonal matrix in (7.6) with the eigenvalues as diagonal, and $\mathbf{A}$ is the original matrix in (7.5). $\mathbf{T}^{-1}$ is found to be

$$\mathbf{T^{-1}} = \begin{pmatrix} -\frac{1}{2\sqrt{1-k^2/3}} & \frac{1}{2} \\ \frac{1}{2\sqrt{1-k^2/3}} & \frac{1}{2} \end{pmatrix}.$$

Using the Crank-Nicolson method on the system (7.6), gives us

$$\hat{x}_{n+1} = \frac{1+\frac{1}{2}\Delta tik\sqrt{1-\frac{k^2}{3}}}{1-\frac{1}{2}\Delta tik\sqrt{1-\frac{k^2}{3}}}\hat{x}_n, \qquad \hat{y}_{n+1} = \frac{1-\frac{1}{2}\Delta tik\sqrt{1-\frac{k^2}{3}}}{1+\frac{1}{2}\Delta tik\sqrt{1-\frac{k^2}{3}}}\hat{y}_n,$$

to use in the numerical procedure. The initial conditions for η and w has to be transformed to the new variables using $\mathbf{T^{-1}}$. When the iterations are done, a transformation back to the original variables w and η is done using $\mathbf{T}$.

Now, it is not enough to rescale the problem to take into account numerical instability. We also have to use a filter, and since the eigenvalues of the problem are complex unless

$$|k| < \sqrt{3}, \qquad \text{since} \quad \lambda = \pm\sqrt{1-\frac{k^2}{3}},$$

we choose a filter so that this is satisfied. The variables have to be filtered after each iteration, and also the initial conditions before the iterations start. With the same discretization as before, we obtain the errors shown in Table 7.3, and the wave profile shown in Figure 7.3

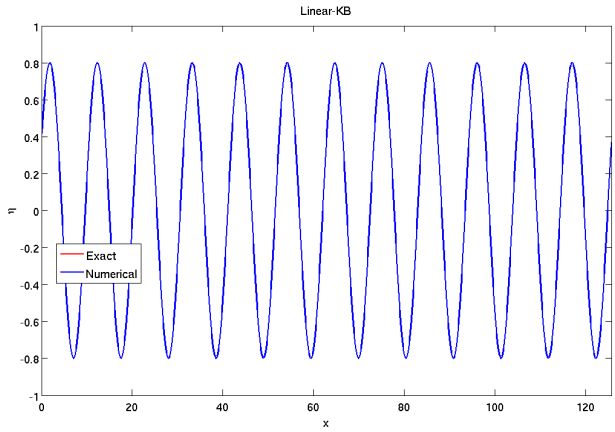

Figure 7.3: Wave profile of the linear part of the KB system for $dt = 0.1$.

	Results for η		Results for w	
dt	L^∞**-error**	**ratio**	L^∞**-error**	**ratio**
0.1000	1.3933e-04		1.4852e-04	
0.0500	3.4844e-05	3.9986	3.7144e-05	3.9986
0.0250	8.7117e-06	3.9996	9.2867e-06	3.9996
0.0125	2.1780e-06	3.9999	2.3217e-06	3.9999
0.0063	5.4450e-07	4.0000	5.8044e-07	4.0000
0.0031	1.3612e-07	4.0000	1.4511e-07	4.0000
0.0016	3.4031e-08	4.0000	3.6277e-08	4.0000
7.8125e-04	8.5078e-09	4.0000	9.0693e-09	4.0000
3.9063e-04	2.1270e-09	4.0000	2.2673e-09	4.0000
1.9531e-04	5.3174e-10	4.0000	5.6684e-10	4.0000

Table 7.3: Errors and ratios for different time steps of the linear part of the Kaup-Boussinesq system.

7.4 The full Kaup-Boussinesq system

Next, we investigate the full Kaup-Boussinesq system

$$\begin{aligned} \eta_t &= -w_x - \tfrac{1}{3}w_{xxx} - (\eta w)_x, \\ w_t &= -\eta_x - \tfrac{1}{2}(w^2)_x. \end{aligned} \tag{7.7}$$

In [11] we find an exact solution of the corresponding KB-system for internal waves, which is already investigated in Chapter 5. We want to compare (7.7) with the KB-system for internal waves

$$\begin{aligned} \eta_t + \alpha u_x + \delta u_{xxx} + \gamma(\eta u)_x = 0, \\ u_t + \beta \eta_x + \epsilon^2 \gamma u u_x = 0, \end{aligned} \tag{7.8}$$

since we have an exact solution for this. We see that if we put

$$\alpha = \beta = \gamma = 1 \quad \text{and} \quad \delta = \frac{1}{3},$$

we have the same system. Now, this gives us the exact solution

$$\begin{aligned} w(x,t) &= \tfrac{2(c^2-1)}{cosh(\sqrt{3(c^2-1)}(x-ct))+c}, \\ \eta(x,t) &= cw(x,t) - \tfrac{1}{2}w^2(x,t) \end{aligned} \tag{7.9}$$

which we will use for comparison to our numerical approach.

7.4.1 Numerical procedure

Transforming our system to the Fourier space, the following system is obtained

$$\begin{bmatrix} \hat{\eta}_t \\ \hat{w}_t \end{bmatrix} = ik \begin{pmatrix} 0 & \frac{1}{3}k^2 - 1 \\ -1 & 0 \end{pmatrix} \begin{bmatrix} \hat{\eta} \\ \hat{w} \end{bmatrix} + \begin{bmatrix} -ik(\hat{\eta w}) \\ -ik\frac{1}{2}(\hat{w^2}) \end{bmatrix}$$

In the same way as we did for the linear part, we diagonalize such that the linear part is not coupled. The eigenvalues of the matrix and the corresponding eigenvectors are the same. We get

$$\begin{bmatrix}\hat{x}_t\\ \hat{y}_t\end{bmatrix} = ik\begin{pmatrix}\sqrt{1-k^2/3} & 0\\ 0 & -\sqrt{1-k^2/3}\end{pmatrix}\begin{bmatrix}\hat{x}\\ \hat{y}\end{bmatrix} + \mathbf{T^{-1}}\begin{bmatrix}-ik(\hat{\eta w})\\ -ik\frac{1}{2}(\hat{w^2})\end{bmatrix}. \tag{7.10}$$

Using again Crank-Nicolson on the linear terms and Adams-Bashforth on the nonlinear, we get the following algorithm

$$\begin{aligned}
\hat{x}_{n+1} &= \frac{1+\frac{1}{2}\Delta tik\sqrt{i-k^2/3}}{1-\frac{1}{2}\Delta tik\sqrt{i-k^2/3}}\hat{x}_n + \frac{\frac{3}{4}\Delta t\frac{ik}{\sqrt{1-k^2/3}}}{1-\frac{1}{2}\Delta tik\sqrt{i-k^2/3}}(\hat{\eta w})_n + \frac{-\frac{3}{8}\Delta tik}{1-\frac{1}{2}\Delta tik\sqrt{i-k^2/3}}(\hat{w^2})_n + \\
&\frac{-\frac{1}{4}\Delta t\frac{ik}{\sqrt{1-k^2/3}}}{1-\frac{1}{2}\Delta tik\sqrt{i-k^2/3}}(\hat{\eta w})_{n-1} + \frac{\frac{1}{8}\Delta tik}{1-\frac{1}{2}\Delta tik\sqrt{i-k^2/3}}(\hat{w^2})_{n-1}, \\
\hat{y}_{n+1} &= \frac{1-\frac{1}{2}\Delta tik\sqrt{i-k^2/3}}{1+\frac{1}{2}\Delta tik\sqrt{i-k^2/3}}\hat{y}_n + \frac{-\frac{3}{4}\Delta t\frac{ik}{\sqrt{1-k^2/3}}}{1+\frac{1}{2}\Delta tik\sqrt{i-k^2/3}}(\hat{\eta w})_n + \frac{-\frac{3}{8}\Delta tik}{1+\frac{1}{2}\Delta tik\sqrt{i-k^2/3}}(\hat{w^2})_n + \\
&\frac{\frac{1}{4}\Delta t\frac{ik}{\sqrt{1-k^2/3}}}{1+\frac{1}{2}\Delta tik\sqrt{i-k^2/3}}(\hat{\eta w})_{n-1} + \frac{\frac{1}{8}\Delta tik}{1+\frac{1}{2}\Delta tik\sqrt{i-k^2/3}}(\hat{w^2})_{n-1}.
\end{aligned} \tag{7.11}$$

The numerical procedure is as follows:

- Transformation of the initial conditions from η and w to x and y
- Filter the initial conditions
- Taking the product ηw and w^2 in physical space, using DFT and transforming it to Fourier space with the inverse DFT
- Filter the products
- For each iteration filter the new x and y, take the new products ηw and w^2 in physical space (having the last ones saved for the $(n-1)$-terms) and filter them
- After the iterations, transform back to the original η and w in physical space.

7.4.2 Results

The numerical results shows that the method works quite well for small amplitude waves, confirming the basis for deriving the model in the first place. It also goes hand in hand with the results of the internal solitary wave discussion from Chapter 4. If the wave speed is chosen to be as small as $c = 1.005$ we get a good approximation with a small error, and we also get the right ratio 4. The results of this is shown in Table 7.4. The wave profile is shown in Figure 7.4.

$c = 1.005$	Results for η		Results for w	
dt	L^∞**-error**	**ratio**	L^∞**-error**	**ratio**
0.1000	2.5936e-08		2.0982e-08	
0.0500	6.4486e-09	4.0219	5.2118e-09	4.0258
0.0250	1.6077e-09	4.0111	1.2988e-09	4.0129
0.0125	4.0135e-10	4.0056	3.2417e-10	4.0064
0.0063	1.0027e-10	4.0029	8.0977e-11	4.0033
0.0031	2.5057e-11	4.0016	2.0235e-11	4.0019
0.0016	6.2619e-12	4.0014	5.0562e-12	4.0019
7.8125e-04	1.5638e-12	4.0042	1.2621e-12	4.0061
3.9063e-04	3.8951e-13	4.0149	3.1381e-13	4.0219
1.9531e-04	9.7469e-14	3.9963	8.0764e-14	3.8856

Table 7.4: Errors and ratio for different time steps of the Kaup-Boussinesq system. Results for η and w.

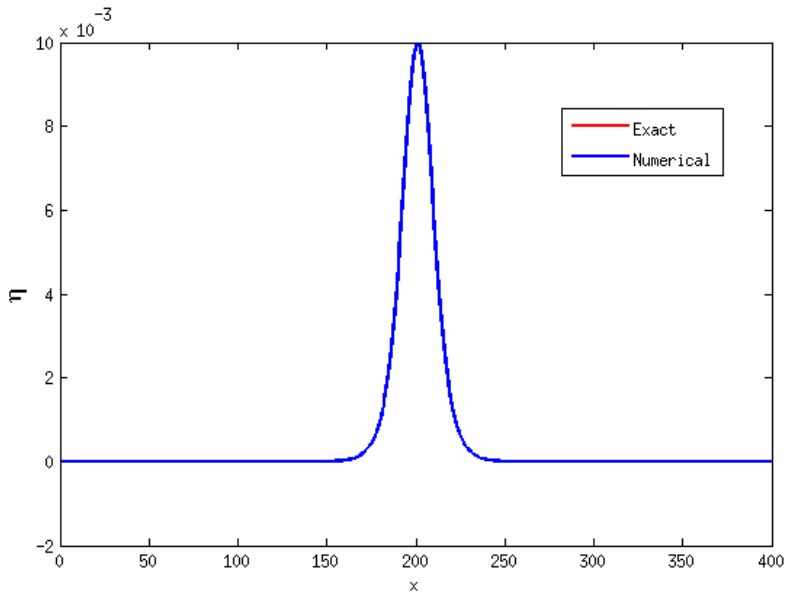

Figure 7.4: Wave profile for $c = 1.005$.

For smaller wave speeds the waves get broader, so we have to increase the length of the interval L to get the error right because of the boundaries. When we increase the wave speed, we can see that some of the energy spreads to the tail and in front of the wave. Nevertheless, the solution seems to be stable up to a certain wave speed. After a certain point the model becomes unstable, and the solution blows up after some iterations. We can see the energy spreading after just $c = 1.2$ and certainly at $c = 1.8$. The wave profiles for these wave speeds are shown in Figure 7.5.

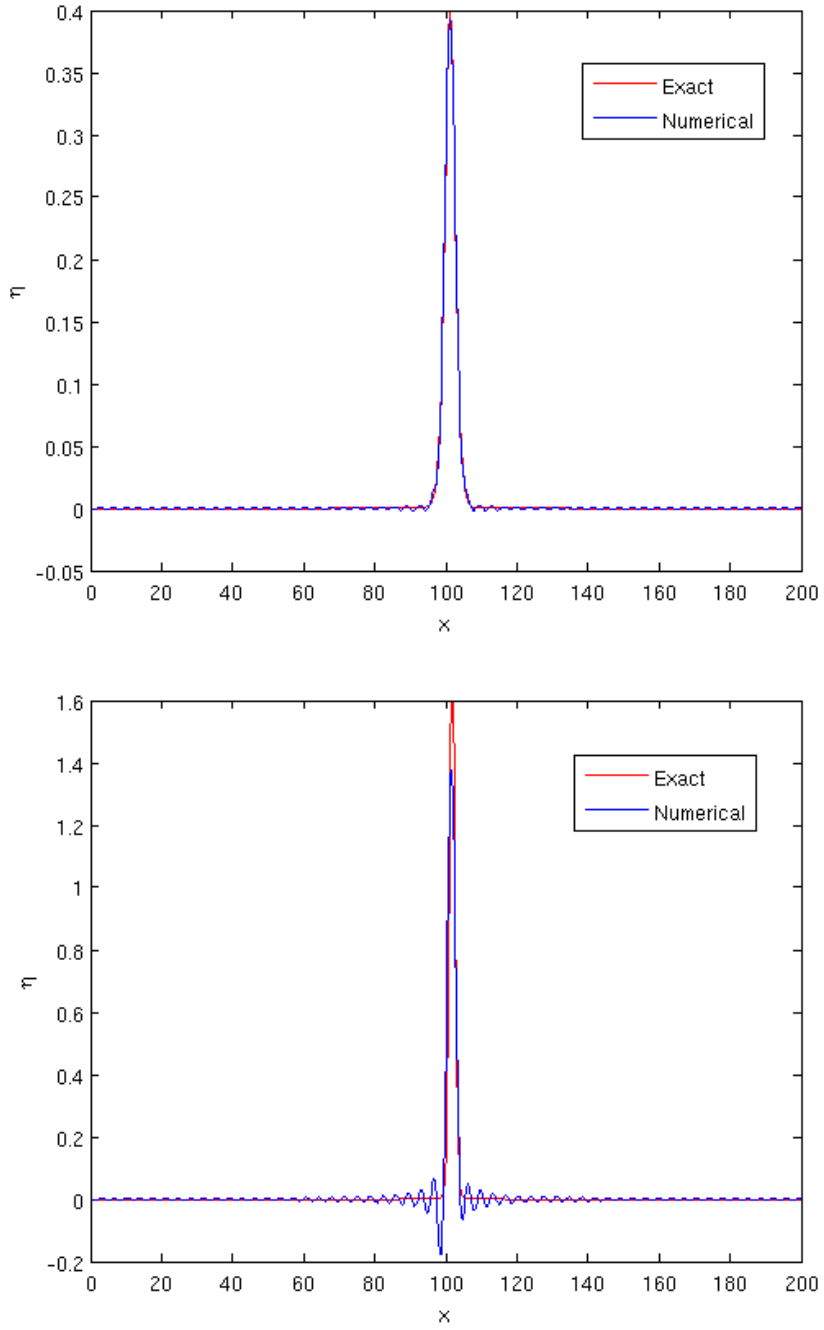

Figure 7.5: Waveprofiles for $c = 1.2$ and $c = 1.8$.

Another thing worth mentioning is that when the products are filtered, we should have some aliasing. One would normally have to use a way to remove this aliasing effect. Here, on the other hand, this was done, and it seemed to

have no effect at all. This could be the fact that a lot of the modes was already filtered out using the requirement $|k| < \sqrt{3}$, and the modes that remained was not enough to produce enough aliasing to take account for.

7.4.3 Conservation of Momentum and Energy

For the interval $[0, L]$, we should have conservation of both momentum and energy, since periodicity is assumed. We use the differential conservation equations of the Kaup-Boussinesq system derived in Chapter 4 to see if this is satisfied with our method. Since these equations are given by w and η, we can use the calculated quantities here. For the momentum differential balance equation, we found

$$\frac{\partial}{\partial \tilde{t}} \tilde{I} = \frac{\partial}{\partial x} F - \frac{\partial}{\partial \tilde{x}} \tilde{q}_I,$$

when terms of order $O(\alpha\beta, \beta^2$ are ignored. Here, the quantities l, c_0, ρ, g and h_0 are put equal to 1, so it does not change when we express it in dimensional variables. We get

$$\frac{d}{dt} \int_0^L I \, dx = \int_0^L \frac{\partial}{\partial t} I \, dx = \int_0^L (\frac{\partial}{\partial x} F - \frac{\partial}{\partial x} q_I) \, dx = F(w, \eta) - q_I(w, \eta) \Big|_0^L = 0,$$

where the derivative is taken inside the integral in the first equality since the interval of integration is fixed, and the last equality is true because of periodicity so that w and η have the same value at 0 and L. Hence,

$$\int_0^L I \, dx = \int_0^L (w + \eta w + \frac{1}{3} w_{xx}) \, dx = \text{constant}.$$

For w_{xx}, we use the computed w and use the Fourier collocation derivative twice. Since we in Chapter 4 use an expression for the energy that satisfies the Hamiltonian corresponding to the KB system, we know that this is conserved for an interval where we have periodicity or the whole real line. This means that

$$\int_0^L E \, dx = \int_0^L (\frac{1}{2}\eta^2 + \frac{1}{2}(1 + \eta)w^2 - \frac{1}{6} w_x^2) \, dx = \text{constant}.$$

These two integrals are evaluated at each time step, and the following plots are time plotted against the integral value. We test conservation with $c = 1.005$. In Figure 7.6 the solution (7.9) is used, and since this is just a translation it is obvious that we have conservation, which we observe from the figure. Thus, we try another initial condition where the numerical solution is clearly different than a normal translation, to see if the method still features conservation. In Figure 7.7 the Gaussian solution

$$w(x, 0) = \frac{1}{10\sqrt{2\pi}} e^{-\frac{1}{2}(\frac{x - L/2 - 0.1}{10})^2} \tag{7.12}$$

is used as initial condition for w For η we simply use

$$\eta(x, t) = A w(x, t), \tag{7.13}$$

where $A = 1.5$ is used for the plot. As can be seen from the figure, the numerical solution is clearly not a translation, but conservation is still satisfied. For both plots, the final time is $T = 25$ with time step $dt = 0.00625$.

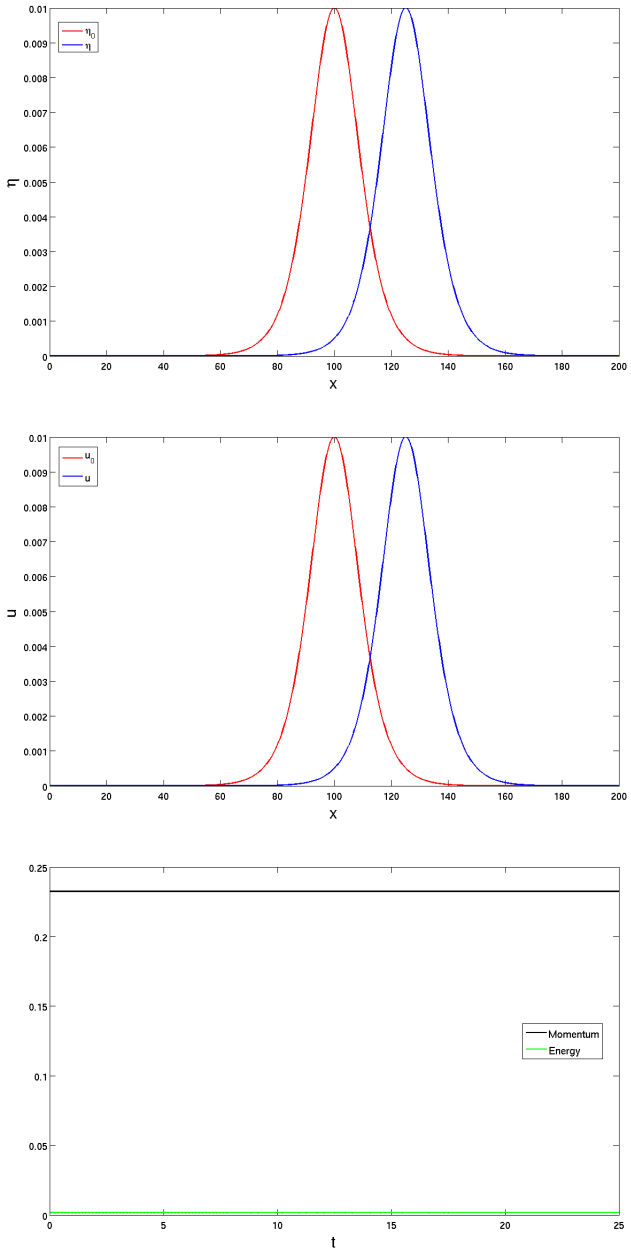

Figure 7.6: Initial condition and numerical solutions for both w and η. The last plot shows the integral of the momentum and energy plotted at each time step. Here, the solution (7.9) is used as initial condition.

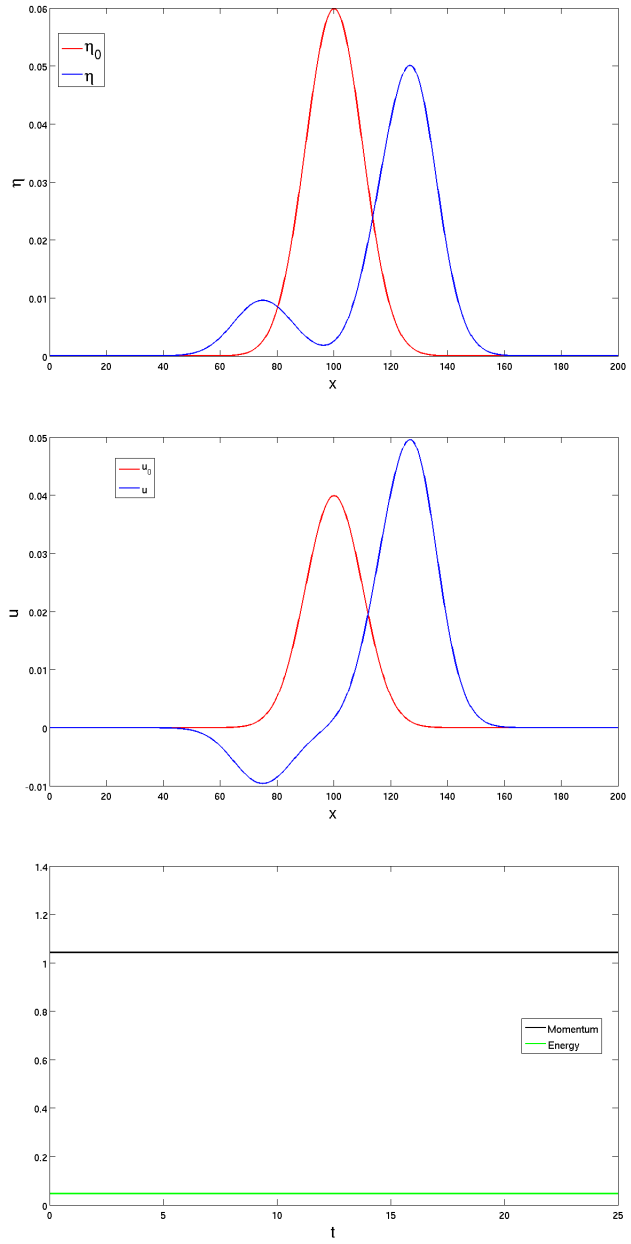

Figure 7.7: Initial condition and numerical solutions for both w and η. The last plot shows the integral of the momentum and energy plotted at each time step. Here, the Gaussian solution (7.12) and (7.13) is used as initial condition.

Bibliography

[1] Ali, A. and Kalisch, H. (2012). Mechanical balance laws for boussinesq models of surface water waves. *Journal of Nonlinear Science*, (Vol 22):371–398.

[2] Ali, A. and Kalisch, H. (2013). Modeling energy conservation in a completely integrable boussinesq system. *Fundamental and Applied Hydrodynamics*, (Vol 6):78–83.

[3] Bona, J. L. Chen, M. and Saut, J.-C. (2002). Boussinesq equations and other systems for small-amplitude long waves in nonlinear dispersive media. i: Derivation and linear theory. *Journal of Nonlinear Science*, (Vol 12):283–318.

[4] Broer, L. J. F. (1974). On the hamiltonian theory of surface waves. *Appl. sci. Res*, (Vol 29):430–446.

[5] Canuto, C. Hussaini, M. Y. Q. A. and Zang, T. A. (1988). *Spectral Methods in Fluid Dynamics*. Springer-Verlag.

[6] Choi, W. and Camassa, R. (1999). Fully nonlinear internal waves in a two-fluid system. *Journal of Fluid Mechanics*, (Vol 396):1–36.

[7] Cohen, I. M. and Kundu, P. K. (2008). *Fluid Mechanics*. Elsevier Inc., fourth edition.

[8] Craig, W. Guyenne, P. and Kalisch, H. (2004). A new model for large amplitude long internal waves. *Comptes Rendus Mecanique*, (332):525–530.

[9] Craig, W. Guyenne, P. and Kalisch, H. (2005). Hamiltonian long-wave expansions for free surfaces and interfaces. *Communications on Pure and Applied Mathematics*, (LVIII):1587–1641.

[10] Grue, J. Jensen, A. R. P. O. and Sveen, J. K. (1999). Properties of large-amplitude internal waves. *Journal of Fluid Mechanics*, (380):257–278.

[11] Guyenne, P. (2006). Large-amplitude internal solitary waves in a two-fluid model. *C.R.Mecanique*, (334):341–346.

[12] Kalisch, H. and Bona, J. L. (2000). Models for internal waves in deep water. *Discrete and Continuous Dynamical Systems*, (Vol 6):1–20.

[13] Kalisch, H. and Nguyen, N. T. (2010). On the stability of internal waves. *Journal of Physics A: Mathematical and Theoretical*, (43):1–12.

[14] Kaup, D. J. (1975). A higher-order wave equation and the method for solving it. *Prog. Theor. Phys.*, (54):396–408.

[15] Li, Y. and Sattinger, D. H. (1998). Matlab codes for nonlinear dispersive wave equations (unpublished).

[16] Ostrovsky, L. A. and Stanton, T. P. (1998). Observations of highly nonlinear internal solitons over the continental shelf. *Geophysical Research Letters*, (Vol 25):2695–2698.

[17] Polking, J. C. (2002). *http://math.rice.edu/ dfield/index.html*.

[18] Whitham, G. B. (1974). *Linear and Nonlinear Waves*. Wiley Interscience.